Atmos. Chem. Phys., 16, 7785–7811, 2016
www.atmos-chem-phys.net/16/7785/2016/
doi:10.5194/acp-16-7785-2016

Atmospheric Chemistry and Physics Open Access EGU

BAERLIN2014 – the influence of land surface types on and the horizontal heterogeneity of air pollutant levels in Berlin

Boris Bonn[1,a], Erika von Schneidemesser[1], Dorota Andrich[1,b], Jörn Quedenau[1], Holger Gerwig[2], Anja Lüdecke[2], Jürgen Kura[2], Axel Pietsch[2], Christian Ehlers[3], Dieter Klemp[3], Claudia Kofahl[3], Rainer Nothard[4], Andreas Kerschbaumer[4], Wolfgang Junkermann[5], Rüdiger Grote[5], Tobias Pohl[6], Konradin Weber[6], Birgit Lode[1], Philipp Schönberger[1], Galina Churkina[1], Tim M. Butler[1], and Mark G. Lawrence[1]

[1]Institute for Advanced Sustainability Studies (IASS), 14467 Potsdam, Germany
[2]Division Environmental Health and Protection of Ecosystems, German Environment Agency, 06844 Dessau-Roßlau, Germany
[3]IEK-8, Research Centre Jülich, 52425 Jülich, Germany
[4]Senate Department for Urban Development and the Environment, 10179 Berlin, Germany
[5]Karlsruhe Institute of Technology, Institute of Meteorology and Climate Research, Atmospheric Environmental Research (IMK-IFU), Campus Alpin, 82467 Garmisch-Partenkirchen, Germany
[6]Environmental Measurement Techniques, University of Applied Sciences, 40474 Düsseldorf, Germany
[a]now at: Institute for Forest Sciences, Albert-Ludwig University, 79110 Freiburg, Germany
[b]now at: Andritz AG, Graz, Austria

Correspondence to: Erika von Schneidemesser (evs@iass-potsdam.de)

Received: 20 January 2016 – Published in Atmos. Chem. Phys. Discuss.: 25 February 2016
Revised: 19 May 2016 – Accepted: 6 June 2016 – Published: 24 June 2016

Abstract. Urban air quality and human health are among the key aspects of future urban planning. In order to address pollutants such as ozone and particulate matter, efforts need to be made to quantify and reduce their concentrations. One important aspect in understanding urban air quality is the influence of urban vegetation which may act as both emitter and sink for trace gases and aerosol particles. In this context, the "Berlin Air quality and Ecosystem Research: Local and long-range Impact of anthropogenic and Natural hydrocarbons 2014" (BAERLIN2014) campaign was conducted between 2 June and 29 August in the metropolitan area of Berlin and Brandenburg, Germany. The predominant goals of the campaign were (1) the characterization of urban gaseous and particulate pollution and its attribution to anthropogenic and natural sources in the region of interest, especially considering the connection between biogenic volatile organic compounds and particulates and ozone; (2) the quantification of the impact of urban vegetation on organic trace gas levels and the presence of oxidants such as ozone; and (3) to explain the local heterogeneity of pollutants by defining the distribution of sources and sinks relevant for the interpretation of model simulations. In order to do so, the campaign included stationary measurements at urban background station and mobile observations carried out from bicycle, van and airborne platforms. This paper provides an overview of the mobile measurements (Mobile BAERLIN2014) and general conclusions drawn from the analysis. Bicycle measurements showed micro-scale variations of temperature and particulate matter, displaying a substantial reduction of mean temperatures and particulate levels in the proximity of vegetated areas compared to typical urban residential area (background) measurements. Van measurements extended the area covered by bicycle observations and included continuous measurements of O_3, NO_x, CO, CO_2 and point-wise measurement of volatile organic compounds (VOCs) at representative sites for traffic- and vegetation-affected sites. The quantification displayed notable horizontal heterogeneity of the short-lived gases and particle number concentrations. For example, baseline concentrations of the traffic-related chemical species CO and NO varied on average by up to ±22.2 and ±63.5 %, respectively, on the scale of 100 m around any measurement location. Airborne observations revealed the dominant source

of elevated urban particulate number and mass concentrations being local, i.e., not being caused by long-range transport. Surface-based observations related these two parameters predominantly to traffic sources. Vegetated areas lowered the pollutant concentrations substantially with ozone being reduced most by coniferous forests, which is most likely caused by their reactive biogenic VOC emissions. With respect to the overall potential to reduce air pollutant levels, forests were found to result in the largest decrease, followed by parks and facilities for sports and leisure. Surface temperature was generally 0.6–2.1 °C lower in vegetated regions, which in turn will have an impact on tropospheric chemical processes. Based on our findings, effective future mitigation activities to provide a more sustainable and healthier urban environment should focus predominantly on reducing fossil-fuel emissions from traffic as well as on increasing vegetated areas.

1 Introduction

Today 54 % of the Earth's population lives in urban areas (United Nations, 2015). This number is expected to increase beyond 60 % within the next 15 to 20 years. Due to the highly concentrated resource use, air pollution levels are closely related to population density, despite some success in reducing emissions (Lamsal et al., 2013). Numerous epidemiologic studies show that highly polluted conditions, such as experienced in many cities, are causing major adverse health effects (e.g., Chen and Kann, 2008; Heinrich et al., 2013; WHO, 2013) that are expected to worsen with increasing urban areas. Therefore it is crucial to find means for improving air quality even under increased urbanization and traffic occurrence, which, however, requires a thorough understanding of sources and sinks of air pollutants.

Poor air quality has been documented in many metropolitan areas such as Beijing (Huang et al., 2015; Huo et al., 2015; Sua et al., 2015; Zhang et al., 2015), Los Angeles (Chen et al., 2013; Ensberg et al., 2014; McDonald et al., 2015), Paris (von der Weiden-Reinmüller et al., 2014) and in Europe in general (Henschel et al., 2015). Elevated levels of gaseous pollutants such as ozone (O_3), nitrogen oxides ($NO_x = NO + NO_2$), sulfur dioxide (SO_2), toxic agents such as aromatic hydrocarbons, and particulate matter (PM) have been attributed to anthropogenic emissions from urban sources, especially traffic and energy production (Downey et al., 2015; Hong et al., 2015; Huo et al., 2015; Padilla et al., 2014). These atmospheric pollutants can affect the human respiratory system (e.g., oxygen capacity) and significantly reduce a person's working capacity and life expectancy (chronic obstructive pulmonary disease, acute lower respiratory illness, cerebrovascular disease, ischaemic heart disease and lung cancer) (CEN, 1993; Dockery et al., 1993; Peng et al., 2005; Pope III et al., 2009; Lelieveld et al., 2015). In this context, oxygen capacity describes the maximum quantity of oxygen that can be transported in a unit volume of blood. This can be used further for the brain and physical work. Air pollution effects on oxygen capacity, work capacity and life expectancy intensify with exposure time and pollutant concentrations. Therefore, daily and annual averages of pollutant concentrations have been proposed by national and international authorities (European Union, 2008; WHO, 2006) and the pollutant concentrations have to be monitored at representative locations for typical daily life conditions, i.e. residential and substantially traffic-influenced sites (Blanchard et al., 2013).

In this context the European Union introduced legally binding limit values applying to all member states in the Air Quality Framework Directive (Directive 2008/50/EC, European Union, 2008). If cities fail to meet these health-related limit values, they are obliged to develop air quality programs capable of reducing the pollution concentration and the duration of elevated concentrations. Establishing such air quality programs is a subjective right of any person directly concerned and can thus be claimed by citizens in court (*Janecek v. Bayern*, ECJ, 2008).

In Germany, the EU limits for NO_2 and PM_{10} continue to be exceeded in many cities (including Berlin). As a result, in drawing up their air quality programs, the Federal Administrative Court ruled that authorities must implement all measures available to keep the time of exceedance as short as possible (Federal Administrative Court, 2012). Otherwise citizens and environmental associations can sue for an adjustment of the program, as has already happened in Darmstadt, Hamburg, Limburg, Mainz, Offenbach, Reutlingen and Wiesbaden.

Berlin, like every European city, has the legal obligation to provide air quality programs that are capable of substantially reducing nitrogen oxides and particulate matter. The Senate of Berlin thereto adopted a clean air program for 2011–2017 (Berlin Senate, 2013b). However, given that limit values continue to be exceeded, it is questionable whether the measures intended are sufficient to enable Berlin to comply with this obligation. An exceedance of these values is only permissible, when all necessary and appropriate measures at disposal are exhausted. So far Berlin has established an environment protection zone (German *Umweltzone*, second step, green level; Berlin Senate, 2011a) in the city center. This measure was intended to lower traffic-related emissions and the annual number of critical threshold exceedances according to EU law for NO_x and PM (see Table 1) in Berlin. It resulted in an emission reduction by 20 % for NO_x and 58 % for soot by diesel engines (Berlin Senate, 2011b). The study by Kerschbaumer (2007) has found a substantial contribution of long-range transport from Polish industrialized areas to local NO_x and PM burden. Several studies (Kiesewetter et al., 2015; Amato et al., 2016) conducted elsewhere supported this claim, while others (Petit et al., 2014; Mancilla et al., 2016) contradicted this finding and identified local

Table 1. European Union (EU) and US (EPA) legislation on selected pollutant concentrations.

	EU		EPA	
Pollutant	daily	annual	daily	annual
Ozone (EU: target value; EPA: limit value)	8 h mean: $\leq 120\,\mu g\,m^{-3}$ ($\approx 60\,ppb_v$) not to be exceeded more than 18 times a year	–	8 h mean: $75\,ppb_v$	–
Nitrogen oxides (NO_2)	1 h mean: $200\,\mu g\,m^{-3}$ ($\approx 100\,ppb_v$) not to be exceeded more than 18 times a year	Mean: $40\,\mu g\,m^{-3}$ ($\approx 20\,ppb_v$)	1 h mean: $100\,ppb_v$	$53\,ppb_v$
Benzene, toluene, xylenes (BTX) compounds	1 h mean: $5\,\mu g\,m^{-3}$ ($\approx 1.9\,ppb_v$)	–	–	–
Particulate matter (PM)	24 h mean: $PM_{10} \leq 50\,\mu g\,m^{-3}$ not to be exceeded more than 35 times a year	Mean: $PM_{10} \leq 40\,\mu g\,m^{-3}$ $PM_{2.5} \leq 25\,\mu g\,m^{-3}$*	24 h mean: $PM_{100} \leq 150\,\mu g\,m^{-3}$ $PM_{2.5} \leq 35\,\mu g\,m^{-3}$	Mean of 3 years: $PM_{2.5,prim.} \leq 12\,\mu g\,m^{-3}$ $PM_{2.5,sec.} \leq 15\,\mu g\,m^{-3}$
Carbon monoxide (CO)	8 h mean: $10\,mg\,m^{-3}$ ($\approx 10.3\,ppm_v$)	–	8 h mean: $9\,ppm_v$ 1 h mean: $35\,ppm_v$ both not to be exceeded more than once a year	–

* Valid from 1 January 2015 onward.

sources to be dominant. Other PM sources than the Polish ones can be attributed to nearby emission or gas-phase (secondary) PM production. As the city of Berlin is surrounded by and contains extensive forested regions, enclosed by three rivers (Havel, Spree and Dahme) and a couple of lakes (6 % by area), the concentration of trace gases and particles will be influenced from both, i.e., local anthropogenic and biogenic (vegetation) sources (see, e.g., Becker et al., 1999; Beekmann et al., 2007).

These vegetative areas are supposed to have notable effects on temperature (Fenner et al., 2014) and air quality. Therefore the increase of green areas such as parks and forests are often considered as measures to counteract urban heat island effects (Collier, 2006; Dousset et al., 2011; Fallmann et al., 2014; Jones and Lister, 2009; Grewe et al., 2013; Schubert and Grossman-Clake, 2013) and air pollution problems (Irga et al., 2015; Janhäll, 2015; UFIREG, 2014). Emission of biogenic volatile organic compound (BVOCs) can affect chemical ozone production and destruction (Seinfeld and Pandis, 2006; Klemp et al., 2012) as well as secondary organic aerosol mass production (Hallquist et al., 2009; Bonn and Moortgat, 2003; Griffin et al., 1999; Sakulyanontvittaya et al., 2008) when higher terpenes are emitted. A high impact of reactive BVOCs on O_3 concentrations and vice versa has been observed during warm seasons in highly polluted temperate and semi-arid areas (Papiez et al., 2009; Bourtsoukidis et al., 2012; Calfapietra et al., 2013; Situ et al., 2013), while the influence in northern countries has been found generally smaller (Setälä et al., 2013; von Schneidemesser et al., 2011). The reducing effect of vegetation on NO_x concentrations was described earlier by Velikova et al. (2005). The effects of vegetation and especially the emission of BVOCs (Guenther et al., 1995, 2006; Ghirardo et al., 2016) have been neglected so far but are expected intensify in a warmer climate (e.g., Bonn, 2014; Churkina et al., 2015).

Given this background, the aim of this study was to identify hotspots of pollution and the variability of basic air pollution trace gases, to quantify the impact of green areas and to exemplarily identify dominant volatile organic compound (VOC) sources to support future development of action plans by the Berlin Senate with improved success.

2 Focus of the campaign and of this study

This study focusses on the Berlin/Brandenburg Metropolitan Region (BBMR), a major European transport hub with about 4 million inhabitants. Both cities in this area, Berlin with approximately 3.3 million citizens and Potsdam, the capital of Brandenburg, with about 0.2 million inhabitants, are extraordinary among European metropolitan areas because of the large proportion of water and vegetated areas that makes up about 40 % of the total land surface area in the cities (Berlin Senate, 2010, 2013b) (Table 2). Because of its large area, vegetation is expected to have a notable impact on pollution levels (trace gas and aerosol particle concentrations),

Table 2. Contribution of different surface types to the total surface area of Berlin.

Surface type	Area covered (ha)	Fraction of total (%)
Built-up areas, streets (19 %)	49 975	56.1
Green areas:	29 275	32.8
forests	16 349	18.3
public green areas	12 926	14.5
Agricultural areas	3953	4.4
Lakes, rivers	5953	6.7
Total	89 157	100

as it was found for other locations (Cowling and Furiness, 2004; Zaveri et al., 2012). While ambient air pollution levels in Berlin generally met the EU limit values within recent years, daily values of nitrogen oxides ($NO_x = NO + NO_2$) and of particulate matter (PM_{10} and $PM_{2.5}$) have not, and they display increasing trends for NO_x. NO_x and particulate matter are responsible for substantial health effects and have a variety of different sources and atmospheric chemical lifetimes and a remarkable spatial heterogeneity, which requires measurement methods of short response times and low detection limits. Because of the large range in particle sizes and the variation in particle composition, several different detection methods such as gravimetry and spectroscopy have been developed and deployed. These methods do not necessarily match for different conditions (Seinfeld and Pandis, 2006) because of different assumptions, such as density, made for the detection. The situation is similar for nitrogen oxides.

Based on previous studies in urban areas, and a limited number of studies in Berlin, the predominant sources of both pollutants are expected to be traffic, residential heating, industry and long-range transport of primary and secondary particulate matter (Seinfeld and Pandis, 2006; Berlin Senate, 2013a, 2015). Earlier studies have indicated substantial deviations between observed and simulated NO_2 (mean: -20 %) and PM values (mean: -10 %) (see, e.g., Tullius and Lutz, 2003), which both influence health (Fischer et al., 2015; Liu et al., 2016) and ozone production (Atkinson et al., 2004; Seinfeld and Pandis, 2006). The deviations of PM are linked to secondary and semivolatile organic substances contributing to particulate mass. These contributions vary depending on ambient mixing ratios of VOC precursors as well as on temperature as the precursors' saturation vapor pressure and the total organic particle mass change, aspects, which are not or poorly represented in air quality models due to their complexity.

Here we present the project "Berlin Air quality and Ecosytem Research: Local and long-range Impact of anthropogenic and Natural hydrocarbons 2014" (BAERLIN2014). Considering the context outlined in the paragraph above, it focused on the following aspects:

1. heterogeneity of particle number concentrations (PNCs) and mass concentrations throughout the city characterized by different sources and sinks including green areas
2. influence of green spaces/areas on urban pollutants (NO_x, VOCs, ozone and particles) levels
3. contribution of anthropogenic and biogenic organic compounds on particulate levels and on ambient concentrations
4. provision of results to support city authorities for future action plan development to improve air quality.

The present study is one of two overview articles on the BAERLIN2014 campaign addressing the mobile observations and analysis, while the second (von Schneidemesser et al., 2016) will focus on the stationary measurements and source apportionment. The investigation of the link between NO_x, different VOCs and secondary organic aerosol (SOA) were split off to a box model study and will also be described in a further article. Aspect (3) is especially of interest for simulation studies when comparing model simulation results with measurements to draw conclusions about PM sources as well as ozone sources and sinks. The aim of this study was to identify hotspots of pollution and the variability of basic air pollution trace gases, to quantify the impact of green areas and to exemplarily identify dominant VOC sources to support action plans such as those made by the Berlin Senate (Berlin Senate, 2013b).

The mobile measurements described in this paper were conducted as part of the larger BAERLIN2014 campaign, which included extensive stationary measurements at an air quality monitoring station in Neukölln, Berlin. The stationary measurements are described elsewhere (von Schneidemesser et al., 2016). Both measurement types contribute to the identification of local sources and sinks as well as their effects on the urban background concentration of air pollutants. Further studies using atmospheric transport models are planned to assess different mitigation options.

3 Methods

Mobile measurements were performed using different observation platforms, i.e., bicycles, a van and aircraft (Table 3), with tracks throughout and around the BBMR area (Fig. 1). To allow for the comparison of different measurement types at different times of day and under different conditions, a relative parameter method has been used, which is described in Sect. 3.4. In order to characterize the spatial variation of parameters of interest, a set of instruments and methods on different platforms were linked to form a complimentary set of observations. The different ranges and scales of observations were as follows.

1. Microscale (Sect. 3.1): this includes variations within street channels, resolution of meters, ground-based,

Table 3. List of applied mobile measurement platforms, parameters quantified and timescales.

Mobile measurement platform	Parameters measured	Timescale
Bicycle	T, particle number concentration, PM_{10}, $PM_{2.5}$, PM_1, PM(health), lung deposited surface area	10 June–5 September
Van	T, RH, O_3, NO, NO_2, CO, CO_2, CH_4, particle number concentration, particle surface area, PM and canister samples (VOCs)	31 July–6 August
Ultralight aircraft	T, dew point, O_3, particle number concentration, particle size distribution	12 June
Airplane (DA 42)	T, dew point, SO_2, particle number, particle size distribution, soot	10 October

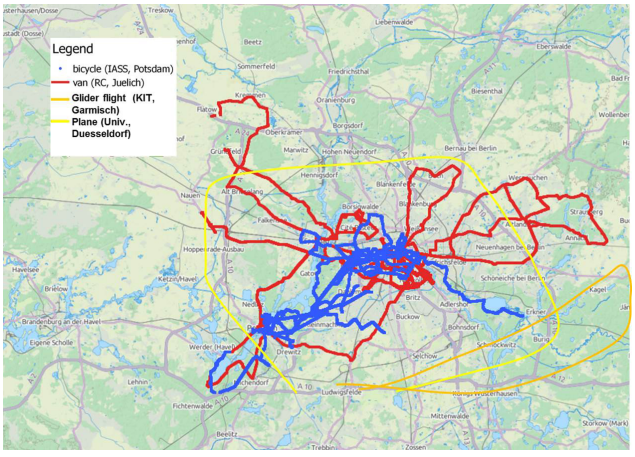

Figure 1. Mobile measurement routes in the BBMR area: bicycle routes in blue, van routes in red and airborne tracks in yellow (air plane) and orange (glider). Berlin is located in the center and Potsdam at the southwestern concurrence of different bicycle and van tracks.

real-time and highly spatially resolved observations; bicycle measurements cover a variety of routes during the 3-month period.

2. Mesoscale (Sect. 3.2): this includes variations within and between streets, resolution of tens of meters, ground-based, including source profiling (traffic and vegetation) and VOC source classification; van (Mercedes VITO) measurements (RC Jülich, Germany) for the first week in August.

3. Mesoscale (Sect. 3.3): variations in the in- and outflow of BBMR area were measured airborne with a resolution of hundreds of meters to kilometers. Two different plattforms were used: (1) ultralight aircraft (KIT, IMK-IFU, Garmisch-Partenkirchen, Germany) for outflow characteristics of BBMR including altitude information and (2) Diamond (DA42) twin-engine small airplane observations (TU Düsseldorf, Germany) circling around Berlin (60 km cycle with Berlin as central point).

The parameters quantified are listed in Table 3, grouped by measurement platform. The different platforms applied different sets of measurement equipment focussing on standard gases (van and airborne) such as CO, NO_x and ozone as well as sensors for particle properties, i.e., sets of number (different size ranges; see Appendix A, Table A1), size distribution and mass (PM_1, $PM_{2.5}$, PM_{10}, PM(alveolic), PM(thoracic) and PM(inhalable)) concentration. The individual setup for the different platforms is provided in the following subsections addressing the individual platforms. All the instruments (see Table 3) were calibrated a priori except the DiSCmini, which was regularly compared with the particle instrumentation at Neukölln (GRIMM 1.108, 5.403, 5.416 and TSI 3350 NSAM) during regular stops about every second day at the reference site (52°29′21.98″ N, 13°25′51.08″ E). Because of different analytical methods (optical, gravimetrical) and size ranges, instruments for quantification of particle mass were compared during the campaign. Therefore, particle instruments of bicycle and van were operated two times for about 2 h in parallel to check for the match of the observations (see Supplement). In case of different time resolution of the instruments, comparisons were done by using corresponding values at identical finishing times of the interval and by averaging both data sets for the coarser time resolution of both. For example, as the GRIMM 1.108 used by the cyclists had a time resolution of 6 s and the ELPI instrument used for the van measurements recorded in time steps of 1 s, the recording time of GRIMM 1.108 was used and compared with the mean of the ELPI measurements acquired during the 6 s beforehand. Further details as to the time frame of measurements, instrument information and all parameters recorded can be found in Tables 3 and A1 in Appendix A. Finally the observations were classified according the predominant land use type (see Sect. 3.5, "Classification of observed data by land use types").

3.1 Bicycle measurements

Bicycles provide a level of flexibility and access to certain areas that cars cannot enter, in addition to their travel speed, which allows for well-resolved horizontal resolution of measurement points. Moreover this measurement type best addresses the conditions where humans are exposed to pollutants. Because of this, they were used as the basic mobile method for the majority of the time period (10 June–29 August 2014). The instruments applied for quantifying meteorological (temperature, relative humidity) and particulate values (number, mass and lung deposable surface area concentrations) are listed with their characteristics in Table A1. In brief, the DiSCmini from Matter Aerosol (CH) was applied for detecting particle number concentrations using a charged equilibrium in the aerodynamic diameter size range of 10–500 nm. More technical information to the instrument can be found in Kaminski et al. (2013). The corresponding software supplied an algorithm estimating the lung deposited surface area, a metric linked primarily to smaller particles and their size distribution providing a measure of potential health effects. We deployed the optical particle counter GRIMM 1.108 (Airing, Germany) for detecting particles in the aerodynamic size range of 0.3–20 µm. The GRIMM 1.108 instrument measured accumulation and coarse-mode aerosol particles with a time resolution of 6 s. It included an additional sensor for air temperature. The inlets of the instruments were kept as short as possible (50 cm each) and were mounted nonflexed at the top of the backpack or pannier, for which an explicit loss correction factor was derived before the start of the campaign (Table S1.1 in the Supplement). Both particle instruments were transported in a backpack or pannier (see Fig. S1.1 in the Supplement) depending on the individual cyclists' preference and noted in a logbook.

This detailed logbook was carried with the instruments and filled out by each cyclist. A Garmin Virb Elite HD action camera with GPS mounted on the handlebar of the bicycle was used to record the exact time and location of the mobile measurement route and facilitate identification of sources. Please find more details on the measurements in Appendix A.

The measurement routes covered large parts of the BBMR area, from southwest to the center, with several repetitions of a number of the routes (see Fig. 1), such as between the Institute for Advanced Sustainability Studies (IASS) in Potsdam and Charlottenburg in Berlin. The majority of the routes followed commuter paths to and/or from the IASS. In total 80 routes, covering 1850 km, were obtained during the 3-month campaign period. The mobile measurements are viewable online at http://baerlin.iass-potsdam.de.

It should be noted that the mobile measurements represent snapshots for a specific location at a certain point in time with substantial influence of local sources and sinks. In addition, scaling to daily and annual time periods is difficult due to the preferred measurement periods in the morning and afternoons, while the sampling frequency in Neukölln was continuous and relatively high. Thus in order to understand the daily pattern of the measured values and all the contributions in detail, microscale simulations would be required. This is beyond the scope of the present study.

3.2 Mobile van measurements

Van measurements were carried out in a 1-week intensive period between 31 July and 6 August using the Research Centre of Jülich mobile laboratory MOBILAB. It consists of a Mercedes Vito van fitted with an isokinetic particle inlet and gas-phase inlets just above the van roof at ca. 2 m above ground level (Ehlers, 2013). The following quantities were measured: temperature, relative humidity, ozone, NO, NO_2, CO, CO_2, methane, total particle number concentration (2.5 nm–3 µm) and size distribution of particles between 7 nm and 20 µm in diameter (ELPI, Decati Ltd., Finland). This ELPI for acquiring the real-time particle size distribution ($\Delta t = 1$ s) uses a corona charger to charge the particles, which are subsequently classified in a 12-stage low-pressure impactor. The particle mass is then calculated for the different size bins (Keskinen et al., 1992). Location data were collected via GPS. A list of the instrumentation is provided in Tables 3 and A1 (Appendix A).

In addition, "baseline" values were derived for CO as well as for the total number and mass of aerosol particles on the local scale measured in real time. These baseline values were running mean values of the lowest 5 % in a running time period of 180 s for minimizing the effect of measurements affected directly by emissions for instance of cars right in front of the van (Ehlers, 2013).

Each day of the intensive period a pre-set route was followed that lasted several hours. The measurement routes started at the IASS in Potsdam and followed cross sections throughout Berlin and its surroundings (see Fig. 1 for more details). Some of the focus areas were industrial areas such as Siemensstadt and Rummelsburg, the Tiergarten tunnel and AVUS for traffic emissions, and various urban green spaces, such as Grunewald, Treptower Park and Pfaueninsel. Please see Table 4 for detailed locations and approximated traffic count rates. In addition to the continuous measurements, canister samples were carried out (see last column in Table 4) and analyzed for VOCs by gas chromatography/mass spectrometry right after returning to Jülich (Ehlers, 2013). Further details of the setup of the van and the analysis methods can be found elsewhere (Ehlers, 2013; Ehlers et al., 2014, 2015; Barker et al., 2006).

3.2.1 Airborne measurements

Due to technical limitations and restrictions of flight permission over Berlin, airborne measurements were carried out at the borders of the investigated region and used to characterize the in- and outflow of particles and trace gases. Two different platforms were applied, each during a separate period. Both

Table 4. Traffic frequencies at selected representative focus areas for canister samples during BAERLIN2014.

Type of area	Area	Location	Traffic frequency (cars day^{-1})	Canister samples collected
Influenced by traffic	Tiergarten tunnel	City center	50 000	10
	AVUS (motorway)	Western Berlin	50 000 to > 80 000	2
Influenced by vegetation	Grunewald	Western Berlin	< 1000 to 50 000	1
	Treptower Park	Southeastern Berlin	20 000	12
	Pfaueninsel	Southwestern Berlin	1000	1

measurement setups are based on long-term experience and included a number of measurements further described below.

The first set of observations was recorded by the KIT ultralight aircraft (Junkermann, 2005; Junkermann et al., 2011, 2016) on 12 June (11:53–14:30 CEST) during the first days of the campaign. The flight originated in Schönhagen (EDAZ), southeast of Potsdam, and followed an eastbound trajectory to Eggersdorf (EDCE) near Fürstenwalde, from which it returned towards Schönhagen for a repetition of the track further to the south (see Fig. 1). Due to the prevalent weather type on that particular day the outflow of Berlin was characterized. The aircraft was equipped with a set of instruments for aerosol number and size distributions, meteorological variables and trace gases (see Table A1; Junkermann, 2005; Junkermann et al., 2011, 2016). The aerosol size distribution instrumentation consisted of a WRAS system, GRIMM (Ainring, Germany) that measured the ultrafine fraction with a scanning mobility particle spectrometer (SMPS + C, GRIMM, model 5.403) in the size range from 4.5 to 350 nm and the fine fraction from 300 nm to 20 µm with an optical particle spectrometer (OPS, GRIMM, model 1.108). The total number of ultrafine particles was measured with a separate fast (1 s) condensation particle counter (CPC4, GRIMM).

The second flight took place on 10 October 2014 (09:30–10:45 CEST) a month after mobile ground measurements had been finished. It was executed by the University of Applied Sciences in Düsseldorf in the context of a measurement campaign at Melpitz, close to Leipzig, organized by TROPOS (Leipzig, Germany). Particle size distributions, particle number concentrations, black carbon (BC), SO_2 as well as temperature and relative humidity were measured from a Diamond (DA42) twin-engine small airplane. Air was sampled using an isokinetic inlet just below the pilots' right window. For details see Weber et al. (2012). Wind conditions on that particular day were as follows: ground level wind speed was 13 km h^{-1} from the southwest and varied between 11 and 33 km h^{-1} on the flight level (see Fig. S2.1 in the Supplement). The flight entered the Berlin area to the southeast and continued at the edge of the inner flight control zone, making a clockwise circle around Berlin (see Fig. 1). Temperature and humidity data loggers (VOLTCRAFT, DL-121TH), a unipolar charger and electrometer (GRIMM, NanoCheck 1320, ultrafine particle number concentration, 25 nm < D_p < 300 nm), an optical particle counter (GRIMM, 1.109, accumulation and coarse-mode particles, D_p > 0.25 µm), an aethalometer (MAGEE, AE 33 Avio, BC), and a sulfur dioxide instrument (Horiba, APSA-370) measured continuously with a time resolution of 15 s (SO_2) or higher. The prevailing wind direction during the flight period was southwest; both inflow and outflow were measured. A complete list of instruments and their time resolutions can be found in Table A1.

3.3 Method for deriving comparable relative concentrations

Over the course of the 3-month campaign, measurements were taken by different platforms, at different locations, under different meteorological conditions and with different time resolution. To make all the data acquired comparable and to facilitate comparison independent of meteorological conditions such as daily maximum temperature, all mobile measurement values were related to the background value of the corresponding parameters at the reference site in Neukölln (von Schneidemesser et al., 2016) at the same time. Previous work on analyzing mobile measurements (e.g., Van Poppel et al., 2013) has required an average background value (reference site). For comparison, Van Poppel et al. (2013) subtracted this background value from the measured value (Van Poppel et al., 2013). The result is a direct marker of local changes with respect to the background site without any possibility for changes by time. Other approaches (e.g., Van den Bossche et al., 2015) subtract the current pollution level at the background site at identical time in addition to the method applied by Van Poppel et al. (2013). Except for temperature measurements, for which we applied the Van den Bossche et al. (2015) approach, we applied the "relative" approach for surface bound observations. The approach was as follows: the individual relative value was calculated by dividing the calibrated mobile measurement by the observation of the same parameter at the reference site at the corresponding time. In order to harmonize the different time resolutions of stationary and mobile measurements, the urban background measurements (reference) were averaged for 30 min intervals to exclude short-term local effects.

In order to calculate relative values the individual mobile observed values were divided by the 30 min averaged stationary measurement values at the corresponding times. In the case of air temperature (in degrees Celsius) this was done by subtraction instead of division as the difference is more representative than the ratio.

$$\Delta X_{\mathrm{rel}} = X(\text{mobile}) / X(\text{reference, MC042 or MW088}) \quad (1)$$

This method yields not the absolute difference, which varies for different meteorological conditions, but the decreasing or increasing percentage compared to the background site (normalization).

The representative reference site was chosen as a permanent urban background measurement station (Shahraiyni et al., 2015a, b) of the Berlin Senate, i.e., the aforementioned Nansenstrasse monitoring network site in Neukölln (MC042; Berlin Senate, 2015). The long-term measurements from this station (container MC042) provided reference data for O_3, CO, NO and NO_2. Additionally, further instruments for the observation of particle properties (mass, number and size) as well as for quantification of selected VOCs were placed in a measurement van (MW088, Berlin Senate) parked at a distance of about 5 m next to the container MC042 in the street at the curb. In this way, a reference was provided against which the mobile measurements could be related to facilitate comparison over space and time. More details on the stationary measurements can be found in von Schneidemesser et al. (2016). While the gaseous measurements always covered identical detection ranges, this was not always the case for particle measurements. Relative particle number concentration ratios (relPNC ($2.5\,\mathrm{nm} < D_\mathrm{p} < 7\,\mu\mathrm{m}$; NanoCPC, van) or relPNC ($10\,\mathrm{nm} < D_\mathrm{p}\,10\,\mu\mathrm{m}$; DiSCmini + GRIMM 1.108, bicycle) vs. $4\,\mathrm{nm} < D_\mathrm{p} < 3\,\mu\mathrm{m}$ (GRIMM 5.416)) were gained from different instruments with different lower cut-off sizes. Due to intense emissions in the urban area and the subsequent coagulation of smaller partially unstable particles, the detection of sizes between 2.5 and 4 nm in particle diameter is usually scarce and the vast majority of particle number is located between 50 and 100 nm. Comparisons of both types at the reference site displayed no significant difference between both observations used for comparison, i.e., the NanoCPC by RC Jülich and the GRIMM 5.416 by UBA.

The resulting data set allowed for the assessment of the van and bicycle measurements at different times and locations to support the identification of different sources and the corresponding regions of impact. All data "relativized" to the Nansenstrasse urban background site in Neukölln will be referred to as the relative values of the urban background reference station.

3.4 Classification of observed data by land use types

The mobile measured data were classified according to the CORINE land use map (Bossard et al., 2000; Waser and Schwarz, 2006; European Environment Agency, 2012). CORINE classifies several tenths of different categories of which 15 land use types representative for the area of interest were extracted and partially lumped. The categories relevant are listed in Table 5. The surface classification had a moderate resolution ($100\,\mathrm{m} \times 100\,\mathrm{m}$) and referred to conditions in 2006 (European Environment Agency, 2012). A data point was associated with the predominant land use type for the grid in which it was located. There were three categories of forested areas (coniferous, deciduous and mixed forests) and two categories for urban residential areas (block arrangements named as "continuous buildings" and single houses named discontinuous buildings) reflecting the effect of dilution and mixing of pollutants. Some of the classes have been grouped with respect to the key aspect of the study, i.e., influence of vegetation on pollutants in urban areas, and to increase the number of data points for statistics. The different agricultural types of CORINE (arable land, pasture and natural grassland) have been lumped to "agriculture". "Parks" and "sport and leisure facilities" have been grouped to urban "green spaces" and, finally, "commercial areas", "transport" and "airport" have been combined to "commercial areas and transport". Once mobile measurement values had been classified, the values were divided by values of identical parameters observed at the reference site in Neukölln at the same time. Results are displayed for classification types with sufficient data (> 100 data points, Wilcoxon test) for analysis using the open R software and its statistics package. Other classification types with partially sufficient data are displayed in shaded colors to indicate tendencies but were not used for detailed discussion. A significant difference of medians of two different categories is considered at 95 % confidence interval using the approach by Chambers et al. (1983) of $\pm 1.58 \cdot \mathrm{IQR}/\sqrt{n}$. IQR is the interquartile range and n stands for the number of data points considered. This formulation is independent of the underlying statistical distribution and is provided in the figures as notches.

4 Results and discussion

The measurement and analysis results and their discussion will be structured as follows: identification of local pollutant level hotspots indicating substantial sources (Sect. 4.1) and presentation of trace gas and particle analysis to elucidate the influence of traffic and vegetation on the observed results (Sect. 4.2). In this way the strong connection between the air pollutants such as CO, NO_x, anthropogenic VOCs and particles with identical sources, such as traffic, will be brought to the fore. This will be used to conclude on the influence of vegetation on urban air pollutant levels in Berlin during summertime (Sect. 5).

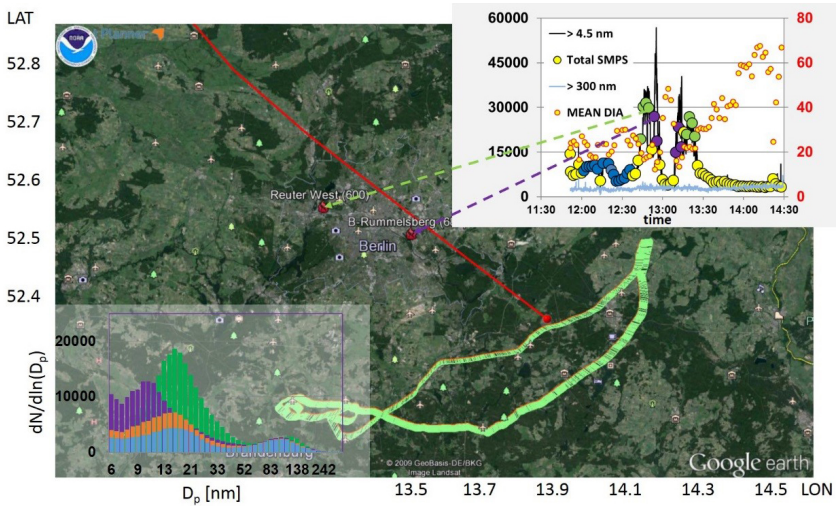

Figure 2. Particle number concentration (particle diameter $D_p > 20$ nm) on 12 June 2014 during the ultralight aircraft measurements (W. Junkermann, KIT, Garmisch-Partenkirchen). Green indicates flight track, white is Berlin city limits, the red line is HYSPLIT back trajectory for the second mamixum (plume), which derived from the power plant in Rummelsburg, and white dotted lines indicate city plume range. Maxima, exclusively in the ultrafine mode, were found in the pollution plumes of the two power plants in Rummelsburg and Reutter-West. The inserts show timeline of particle number concentrations (cm^{-3}) from CPC (black line), SMPS, large dots, fine particles > 300 nm (grey) (cm^{-3}]) and geometric mean diameter (nm), (small dots) and size distributions within city and power plant plumes.

Table 5. Land use types based on the CORINE classification. For number of measurement values (n) for each surface type for each instrument/parameter, see the Supplement.

No.	Surface type name	Surface character type
1	Urban (continuous buildings)	Residential areas, block houses with several floors
2	Urban (discontinuous buildings)	Residential areas, single houses, less dense setting
3	Industry	Industrial area
4	Commercial and transport	Commercial areas, streets, railways, motorway, airport
5	Green spaces	parks, sporting facilities with vegetation
6	Agriculture	Arable land, pasture, grassland
7	Forests (deciduous)	Deciduous forests
8	Forests (coniferous)	Coniferous forests
9	Forests (mixed)	Mixed forests

4.1 Identification of local pollutant hotspots

Comparing pollution levels in- and outside the city area of Berlin has been used to distinguish between local sources and long-range transport contributions. Approaching Berlin by aircraft at 500 m a.g.l. (11 October) (upper mixing layer) around 11:00, SO_2 volume mixing ratios were observed fairly low (≤ 1.5 ppt_v). Total particle number concentrations ($PNC_{4.5}$) between 4.5 and 300 nm in diameter (D_p) were measured close to 2500 particles cm^{-3} ($PNC_{4.5}$ displayed as UFP, Fig. 2) at the upwind edges of the city area and increased to value between 9000 and 12 000 cm^{-3} downwind, i.e., subsequent to its passage of the Berlin city plume. These city plume values measured aloft were found to agree with the ones found at the surface at the urban background site in Neukölln (PNC_{10}, 8800 ± 5000 cm^{-3}, $D_p > 10$ nm) during the summer campaign, indicating a similar atmospheric composition and a minor contribution of particles between 4 and 10 nm and above 300 nm in aerodynamic particle diameter aloft. Similar findings as in October for $PNC_{4.5}$ have been made for total particle number concentrations (PNC_{20}, $D_p > 20$ nm) on 12 June (ultralight aircraft flight) at an elevated flight level of about 1500 m a.g.l. Both flights detected maximum ultrafine and total particle number concentrations when the sampled air plume crossed one of two power plants, (P1) Reutter-West (600 MW), north of the Olympic Stadium in Charlottenburg (west, 52°32′6.25″ N, 13°14′30.59″ E), and (P2) Klingenberg (680 MW), in Rummelsburg (east, 52°29′24″ N, 13°29′42″ E), prior to the sampling. The plume pathway was derived from HYSPLIT (Draxler and Rolph, 2013) and observed cloud base temperature. In June the PNC_{20} concentrations exceeded values of 35 000 and 45 000 cm^{-3} in the corresponding P1 and P2 plumes, while concentrations declined to 3300 cm^{-3} upwind of Berlin. The substantial variation in time and the match of the measurements with plumes affected by the power plants displaying elevated levels of BC and SO_2 provided confi-

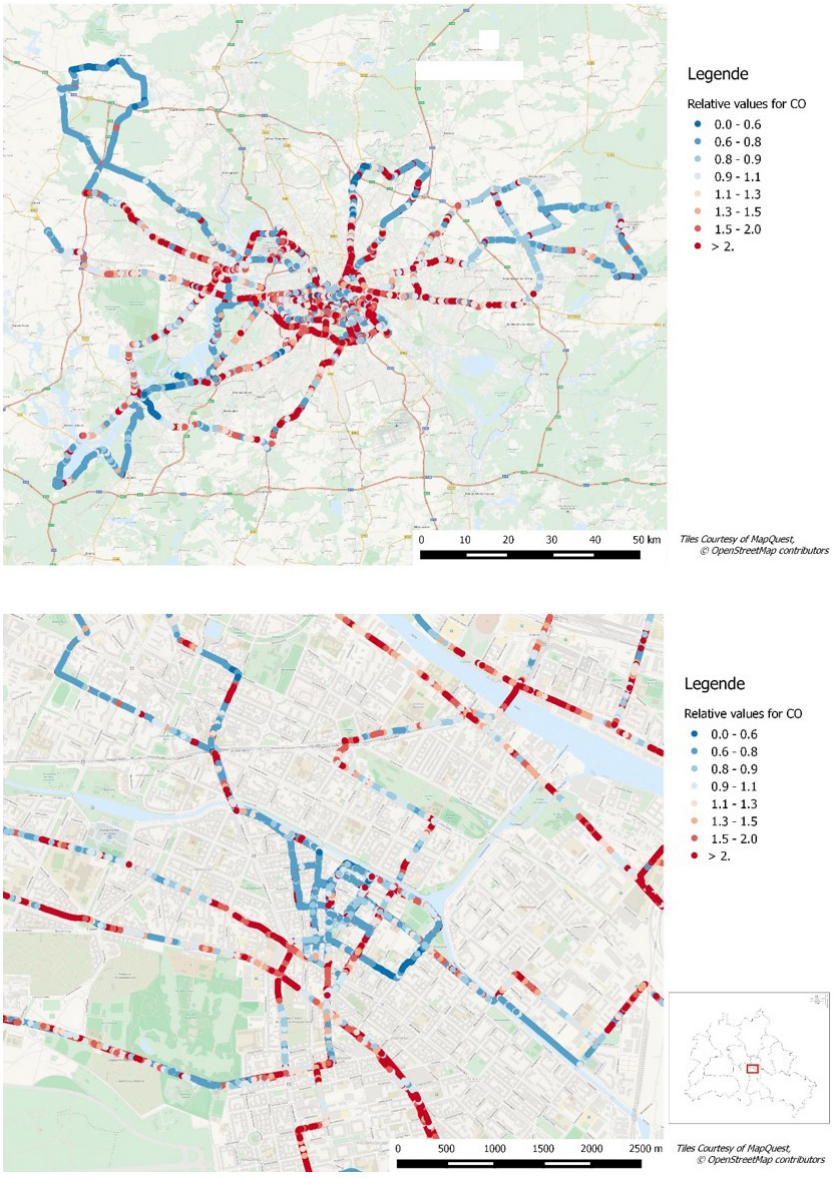

Figure 3. Relative values observed for carbon monoxide in the entire area of study (top) and specifically in Neukölln (bottom). Colors indicate the horizontal heterogeneity and the deviation to the reference in Neukölln. White dots indicate matching values ±10 % the measurements at the reference site.

dence about a notable contribution of those aloft. These observations suggest a similar background level of different PNCs for the majority of the mixing height except close to pollution sources.

Flight level PM mass concentrations were substantially lower (PM_{10}: ca. 8 µg m^{-3}, $PM_{2.5}$: ca. 6 µg m^{-3}) than at the surface in Neukölln (BLUME 042) (PM_{10}: 20–25 µg m^{-3}). However, PM_{10} concentrations at flight level were similar to concentrations observed at the city boundary on the flight day at measurement stations in Grunewald (west) and in Friedrichshagen (southeast) with notable traffic rates and values between 9 and 10 µg m^{-3} (BLUME, von Stülpnagel et al., 2015). Moderately elevated mean concentrations of 16 µg m^{-3} were only observed at the surface measurement stations (BLUME, von Stülpnagel et al., 2015) and at flight level (15 µg m^{-3}, this study) in the northeast of Berlin, close to Buch and Bernau, which was downwind of the city.

Concerning the background contributions Berlin caused a 2- to 3-fold decrease of PNC values at flight level on the 10 October 2014 in ultrafine particle concentration (UFP, 25 nm < D_p < 300 nm) (see Figs. 3 and S2.1) behaving the opposite to PM (2-fold increase). As PM provides substantial particle surface area it would enhance the so-called condensation sink, i.e., reduction of the lifetime of condensable

species and uptake is preferred over new particle formation (Kulmala et al., 2001; Lehntinen and Kulmala, 2003). This clearly indicates that the majority of PM sources are found within the city boundaries at the measurement conditions during summertime (Figs. 2, 4, S4.4 and S4.5). Based on the flight measurements it can be stated that particle number concentrations displayed a regionally applicable background standard and enhanced clearly at notable sources, while PM concentrations were evidently height dependent.

The variation of different PNC and PM intensified at the surface, which can be seen in Fig. 5 with PNC_3 ($D_p \geq 3$ nm, van) and PNC_{10} ($D_p \geq 10$ nm, bicycle) as well as PM_{10} for both van- and bicycle-based observations. Both platform-based observations were directly compared during two parallel tracks of more than 90 min each with the van following the cyclist at street level in order to exclude the van's exhaust. The comparison on 4 August is shown exemplarily in Fig. 6. Two graphs are shown; the left one displays total particle number concentration (bicycle: PNC_{10}, DISCmini ($10\,\text{nm} < D_p < 500\,\text{nm}$) + GRIMM 1.108 ($500\,\text{nm} < D_p < 20\,\mu\text{m}$); van: PNC_3, nanoCPC ($2.5\,\text{nm} < D_p < 3\,\mu\text{m}$) + ELPI ($3\,\mu\text{m} < D_p < 10\,\mu\text{m}$), see Table 3) and the right one presents the particulate mass values observed below 10 µm in diameter (GRIMM 1.108 ($D_p > 270$ nm) vs. ELPI, ($D_p > 30$ nm), Table 3). The van measurements of particulate mass were considered twice, i.e., all the measurements and the lowest 5 % (bg = baseline) in a moving 3 min period to exclude peak values. Note the different heights of the inlets for the van around 2 m a.g.l. (Ehlers, 2013) and cyclist measurements at about 1 m a.g.l., which influenced the results very close to the sources. While the baseline values, i.e., NanoCPC and DISCmini for number concentrations and GRIMM 1.108 and ELPI for PM_{10}, measured by the different platforms agreed within the uncertainty range, peak values showed only a moderate agreement. This was presumably caused by short-term pollution drops, i.e., strong horizontal and vertical changes, as measurements were performed next to the location of particle number formation with rapid particle dynamics and associated growth processes. Moreover, both platforms were not always able to drive right next to each other because of traffic density and changing lanes. As can be seen in Fig. 6 on the left the comparison of both total number measurements of the van, i.e., NanoCPC and ELPI (both van), disagreed in magnitude because of the different cut-off limits of both instruments. While the upper limit was less critical for total number concentration, the major effect was caused by the difference in lower detection limit with 3 nm for NanoCPC, 10 nm for the DiSCmini and 30 nm for the ELPI with respect to the lowest particle diameter detectable. As freshly formed new particles from traffic are expected to appear at sizes below 30 to 40 nm in diameter the notable gap between DiSCmini and ELPI instruments became important (Fig. 6, left plot). With respect to total aerosol mass, displayed here as PM_{10}, the van results (ELPI)

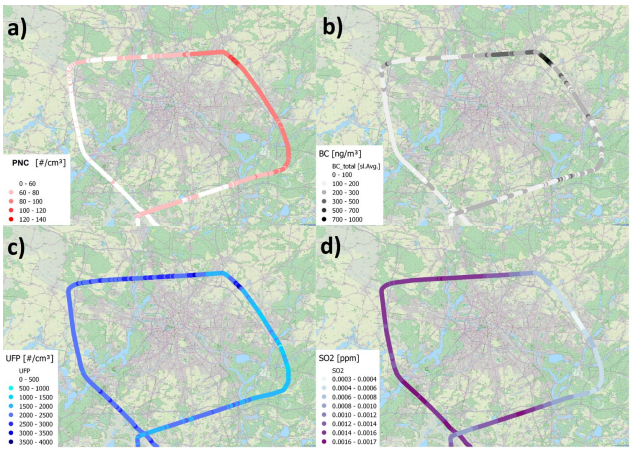

Figure 4. Spatial distribution of the air plane measurements on 10 October 2014: **(a)** coarse particle number concentration, **(b)** BC, **(c)** ultrafine particle number concentration and **(d)** sulfur dioxide.

are slightly higher than the bicycle observations (GRIMM 1.108). Baseline values were enriched by 16.4 ± 0.1 % and all values measured by 58.1 ± 0.2 %. This can be traced back to the different detection range of both instruments with the ELPI, including particle masses between 0.03 and 0.3 µm the GRIMM 1.108 does not cover, and the different time resolution: $\Delta t(\text{ELPI}) = 1$ s and $\Delta t(\text{GRIMM 1.108}) = 6$ s.

While the particle measurements of different platforms agreed well, the observations in different environments and at different land use types did not always (PNC in Table 6 and PM_{10} in Table 7). Details for further parameters such as PM_1 or health-related PM can be obtained from the supporting online information. Especially in traffic-affected areas such as motorways (AVUS), Hardenbergplatz (Tiergarten, Berlin, next to the central bus stop Zoologischer Garten) and larger crossings, the bicycle-based observations, conducted either on the pedestrian path or on a special bicycle track, were substantially lower than the values observed by the van on the street. Relative values used for indicating local sources covered a large range: relative PNC values found for the van measurements ranged from about 30 % of the urban reference value outside of the area of Berlin to the 85-fold in areas with substantial traffic density and in street canyons with less ventilation. Peak values exceeded the 200-fold concentration of the reference site. The hotspots appeared at motorways and the primary entering routes into Berlin, i.e., Hohenzollerndamm, Hasenheide, Karl-Marx-Straße and the neighboring streets in Kreuzberg and major crossings such as the Hardenbergplatz (Zoologischer Garten). The largest value of the entire campaign was recorded by a cyclist passing a waiting double decker bus at a bus stop ($PNC > 10^6\,\text{cm}^{-3}$), indicating conditions that waiting passengers face at a bus stop.

Similar patterns but much more moderate increases have been seen for particulate masses. This can be explained as follows: as remarkable fractions of particle mass are of

Table 6. Particle number concentrations (bicycle/van (background) measurements) for different land use types in particles per cubic centimeter. "–" indicates areas which have not been tested by the method. This table provides the 25th, 50th and 75th percentiles as well as the mean and the number of available data points.

Surface type	25th	Median	75th	Mean	No. of data
Urban block buildings	8589/7555	13 050/10 110	21 160/32 915	25 860/13 390	55 132/21 646
Urban single buildings	6021/4550	9490/6181	15 400/10 080	17 040/8861	139 597/81 293
Industry	6269/7201	8624/10 614	16 220/16 710	16 990/14 488	9966/13 784
Commercial areas and transport	5918/9219	8553/13 780	14 810/18 850	14 390/17 069	4367/4856
Green spaces	4718/6441	7270/8854	11 527/16 500	12 990/14 828	14 493/10 287
Agriculture	–/2967	–/4869	–/7072	–/7200	–/9271
Deciduous forest	3646/3846	4991/5467	10 620/9169	8657/11 865	28 726/8806
Coniferous forest	3613/3501	5802/4993	8394/5658	12 192/14 630	38 485/7020
Mixed forest	3828/3501	6059/5093	10 520/7685	11 687/11 865	7215/1810

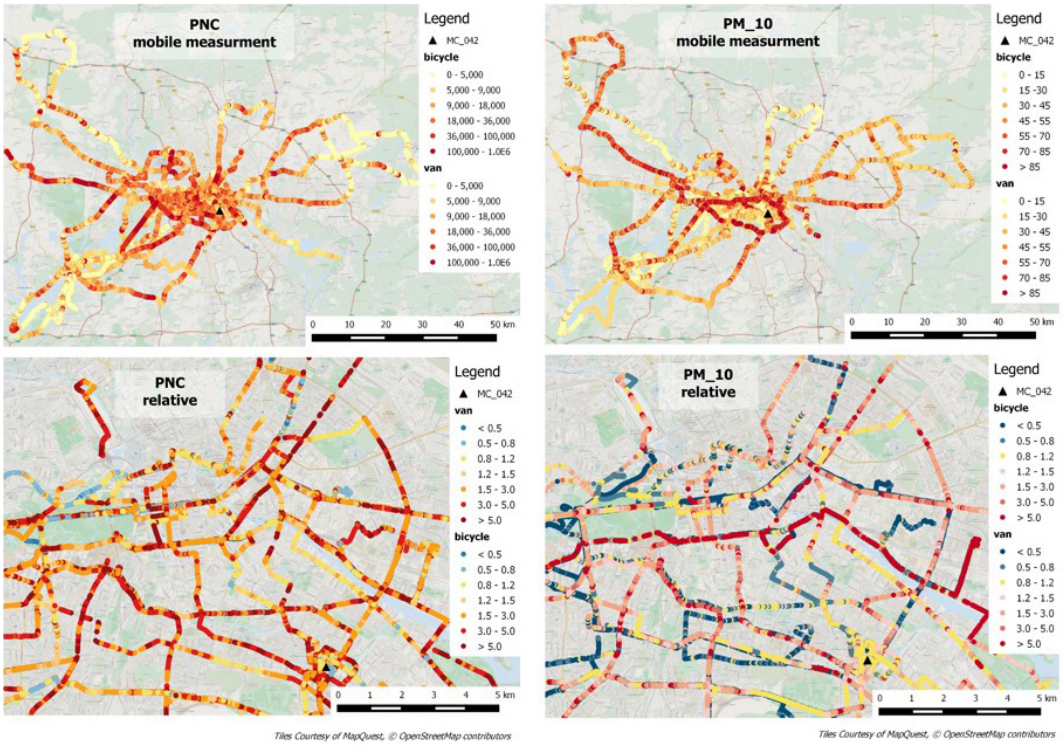

Figure 5. Heterogeneity of particle number (left) and mass (PM_{10}, right) concentrations in and around Berlin detected by bicycle and van sensors. The upper line displays the total area and the bottom line provides the relative values for number and PM_{10} concentrations.

secondary organic origin (mass closure at reference site in Neukölln: 38 ± 9.4 %; Kofahl, 2012; von Schneidemesser et al., 2016), new particle formation and particle mass production require different process times and sink strengths. Consequently, depending on source strength, the observed relationship between source and PM may result in a smeared picture in the vicinity (tens of meters) of sources, with greater enhancement for particle numbers.

The dominant impact of traffic sources on ambient pollutants was seen in the gas-phase measurements of CO, NO_x and ozone at the surface, too. While urban CO may originate to a smaller extent from photochemistry (Finlayson and Pitts Jr., 2000; Atkinson et al., 2004, 2006) and atmospheric transport, its dominant urban source is incomplete combustion of fossil fuels (Klemp et al., 2012). This is indicated in Fig. 3 in blue for the entire area investigated (top) and zoomed in on southern Berlin (bottom). Several locations had elevated mixing ratios and relative values: (i) the Tiergarten tunnel with accumulation of pollutants and substantial amounts of traffic, (ii) Straße des 17. Juni across the Tiergarten and its continuation as Unter den Linden with a significant number of public transport and tourist busses and older

Table 7. Particle mass (PM_{10}) burden characteristics (bicycle/van background (van all) measurements) at different land use types in $\mu g\,m^{-3}$. "–" indicates areas which have not been tested by the method. This table provides the 25th, 50th and 75th percentiles as well as the mean and the number of available data points.

Surface type	25th	Median	75th	Mean	No. of data
Urban block buildings	6.9/12.2(17.4)	13.6/17.2(32.8)	22.7/31.8(74.7)	24.3/25.7(75.6)	8260/21 801
Urban single buildings	7.9/14.2(18.6)	15.0/24.3(34.3)	25.2/38.0(69.4)	29.0/28.7(67.9)	19 143/82 502
Industry	13.6/16.8(19.6)	23.9/26.1(35.9)	36.5/34.9(72.2)	30.7/28.2(73.9)	1464/14 047
Com. + transp.	7.4/28.3(39.5)	13.3/34.8(53.4)	23.4/39.7(77.9)	19.8/35.8(84.1)	478/5613
Green spaces	5.0/13.0(16.4)	9.9/17.9(31.1)	17.1/33.5(59.7)	18.5/25.8(73.2)	2987/12 976
Agriculture	–/13.3(17.8)	–/26.1(29.5)	–/29.1(46.0)	–/24.2(48.3)	–/10 788
Deciduous forest	2.8/14.4(19.1)	5.9/21.0(38.0)	10.4/43.7(71.4)	8.9/29.1(58.2)	2096/8874
Coniferous forest	3.2/12.4(17.8)	7.1/21.9(38.3)	12.6/47.7(70.9)	12.7/30.3(52.7)	4141/7078
Mixed forest	3.4/13.1(15.8)	7.8/18.7(32.7)	13.5/45.0(65.9)	13.8/27.2(53.6)	694/1820

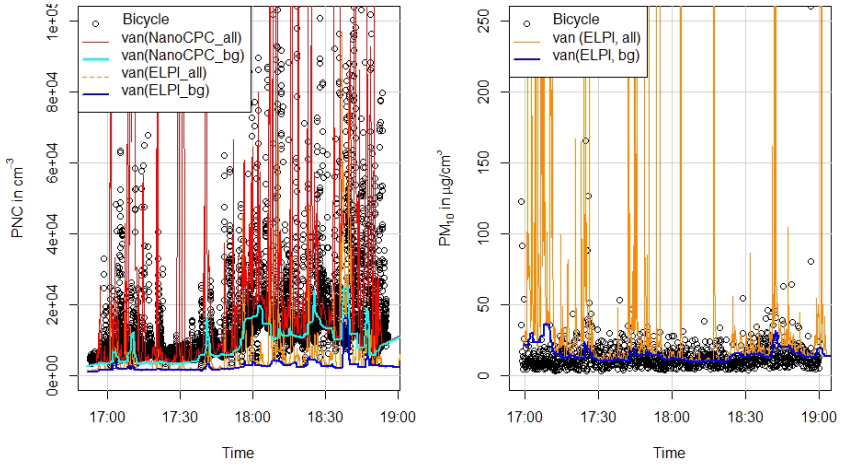

Figure 6. Comparison of bicycle and van-based particle measurements: (left) total particle number concentration and (right) PM_{10} mass, on 4 August 2014. Van measurements are shown by the two colored lines, with the red line representing all measurements and the blue line the calculated background concentrations (10th percentile of 3 min running mean). The time is provided in CEST.

vehicles, the major traffic routes such as (iii) Frankfurter Allee (east), (iv) Mehringdamm (south), (v) Westkreuz and (vi) AVUS (west), as well as (vii) around the central station. The individual locations are indicated in Fig. S3.1.1 as far as they are included in the area of the plot. Mobile measured values ranged between 100 ppb_v and 43.8 ppm_v for CO (all values) and between 100 ppb_v and 3.8 ppm_v for CO (baseline), evidently showing the major source to be traffic related. Median mixing ratios for NO and NO_2 ranged between 5.6 and 0.7 ppb_v in more remote locations with little traffic and between 2.1 ppm_v NO and 2.9 ppm_v NO_2 in locations characterized by significant traffic. This includes in some cases traffic hubs at the intersection of major roads coinciding with bus terminals and other public transport infrastructure, e.g., Hardenbergplatz near Zoologischer Garten. These findings agree with the results of Tullius and Lutz (2003) that NO_x in the BBMR is emitted primarily from vehicles, specifically fossil-fuel-based internal combustion engines. Figure S3.1.1 in the Supplement displays the horizontal variation in mixing ratios of NO and NO_2 (top), as well as the relative values (bottom). The relative values ranged from 0.5 to 4000 for NO and 0.2 to 500 for NO_2. The named hotspots and key travel routes (see above) strike out in absolute mixing ratios and relative values (Figs. 3 (CO) and 7 (ozone)). Crossings displayed substantially elevated mixing ratios of CO and NO_x, which will be part of a follow-up study.

While CO and NO_x increase, ozone volume mixing ratios decreased in the presence of elevated NO_x (presumably by titration with NO) although the effect gets distributed over a larger area. The AVUS motorway and the Tiergarten tunnel with high amounts of fossil-fuel-consuming vehicles (see Table 4) strike out. The VOC matrix become much more complex. As mentioned above exemplary canister samples were taken at representative sites for traffic- and vegetation-affected conditions and analyzed in Jülich. The corresponding results will be presented in the following Sect. 4.2. They strongly support the findings described for particle properties and basic trace gases. The next key aspect is the influence of

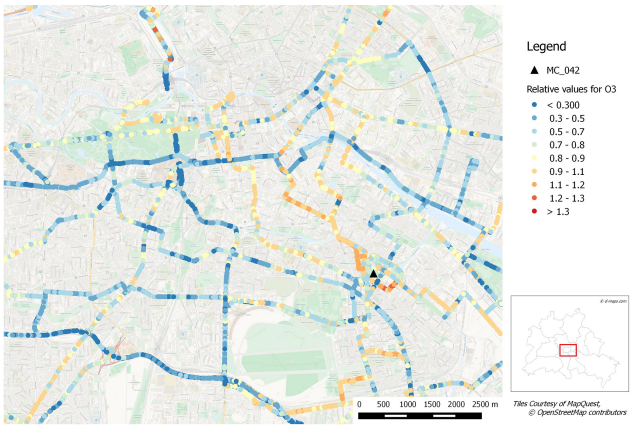

Figure 7. Horizontal variation of relative ozone mixing ratios, i.e., measured values relative to the ones at the same time in Neukölln. As before, white indicates less than 10 % difference to the reference site.

vegetation and its VOC emission and uptake of pollutants in the urban area.

4.2 Impact of vegetation on air pollutant levels

A variety of tools were used to evaluate the impact of vegetation on air pollution levels throughout the city, including (1) canister air samples for VOC analysis taken at different hotspots of traffic-dominated (anthropogenic) and vegetation-dominated (biogenic) emission-related sites in Berlin as well as (2) the classification of the acquired data according to the CORINE land use types described above.

Canister samples include two locations dominated by traffic emission (AVUS motorway and Tiergarten tunnel), three locations dominated by biogenic emissions (Grunewald, Treptower Park and Pfaueninsel) and one location for the representative urban background condition in Neukölln with both trees and minor amounts of traffic within the next 150 m. A one-off sample was taken in the vicinity of a leaf blower being used, which is a common method for cleaning the pavements. This will be used for interpretation of observations made in residential areas, where a running leaf blower was turned on and may have affected the measurements (Table S2.1). All compounds analyzed (Table 8) were considered to be representative for conditions at background level, where no direct emission sources were expected, e.g., toluene mixing ratios in vegetation dominated areas and isoprene and monoterpenes in traffic dominated areas. In both tables results were marked as anthropogenically affected in bold, if the monitored VOC concentrations exceeded the background level, i.e., the level of vegetated areas unaffected by direct emissions of the corresponding compound (average of the two locations with the lowest mixing ratios $+ 2 \cdot$ standard deviation). The corresponding results at with a substantial impact of BVOCs were underlined.

In general, the mixing ratios of anthropogenic VOCs (AVOCs) observed at the AVUS (motorway in the western part of Berlin) were substantially higher than for all the other sites, e.g., within the Tiergarten tunnel (city center), Nansenstrasse (reference site) or Grunewald. A compound concentration specific ratio of a selected location/reference site larger than unity (= enhancement) was found between 2 and 27 for non-biogenic species, depending on the individual species. The sample results show substantially elevated (significance level of ± 5 %) levels of smaller alkanes, alkenes and alkynes such as ethane, butane, propene, ethyne and propyne (Table 8). As expected from previous studies (e.g., Caplain et al., 2006; Stojić et al., 2015; Valach et al., 2015), typical aromatic compounds like benzene, toluene, trimethylbenzenes (TMBs), ethylbenzene and xylenes, as well as several alkanes and alkenes, methyl butene and ethanol, were present in high quantities. Those compounds are related to fossil-fuel consumption and are released either by incomplete combustion or by volatilization from fuel tanks (Jedynska et al., 2015; Schmitz et al., 2000). Ethanol can be related to the increased usage of bioethanol in E10 fuel (10 % of ethanol). The situation is similar within the Tiergarten tunnel, although the AVOCs were on average only 38 ± 29 % of the concentration levels at the AVUS. The ratio VOC(Tiergarten tunnel) / VOC(AVUS) is lowest for the most reactive species (alkenes such as butane and TMBs, 14–17 %) and highest for general oxidation products of tropospheric chemistry (e.g., methanol 91 %). Two exceptions were butanol and cyclopentane with +130 %, indicating different sources or a different car fleet within the center of Berlin controlled by the *Umweltzone*, while independent investigations on vehicle identification numbers did not show a significant change in car types (Berlin Senate, 2011b). Further information about the effect of the Berlin *Umweltzone* can be found elsewhere (Berlin Senate, 2011a).

As a first conclusion it can be stated that the vegetation-related sites (Grunewald, Treptower Park and Pfaueninsel) showed elevated influence of AVOCs the closer and the more intense the nearest traffic sources were. This was especially evident at Treptower Park with more than 200 ppt_v of benzene and 275 ppt_v of toluene. In contrast, significant mixing ratios of BVOCs and corresponding oxidation products such as methanol, acetaldehyde and acetone (MacDonald and Fall, 1993; Warneke et al., 1999; Kreuzwieser et al., 2000; Hüve et al., 2007; Folkers et al., 2008; Holst et al., 2009) were identified as contributing significantly to the total VOCs and oxidation capacity present in the entire BBMR (Bonn et al., 2016); thus vegetation influences urban air quality to a notable extent. For investigation of this the urban reference site at Nansenstrasse was found as a good representative site located in between both extremes, i.e., traffic- and vegetation-affected sites, displaying substantial contributions of both.

This was used for classifying the median conditions at different land use types to recognize the impact of vegetation and traffic sources on the ambient air pollution levels and

Table 8. Canister samples analyzed for VOC compositions. An ozone scrubber was applied in front of the inlet to prevent sampling losses and artifacts. All values are provided as mean volume mixing ratios in ppt_v. The different environments are grouped and the number of available samples is provided for each case. The third column represents urban background measurement conditions at Nansenstrasse (urban background standard). Elevated anthropogenic compounds with respect to vegetated background area concentration (> average + 2 SD of the two smaller mixing ratios of vegetated areas) are marked in bold. Underlined numbers mark biogenic compounds exceeding the average of the two smaller mixing ratios for anthropogenic dominated areas ± 2 standard deviations. Marked numbers represent the compounds substantially affecting the area with no predominant emissions. b.d. abbreviates below detection limit.

Compound	Locations dominated by engine-related emissions		Urban background	Locations dominated by biogenic emissions		
	Motorway, traffic jam 2 samples	Tiergarten tunnel 10 samples	Nansenstrasse 14 samples	Pfaueninsel 1 sample	Treptower Park 11 samples	Grunewald 1 sample
Ethene	**16 973 ± 1262**	**5113 ± 1257**	**465 ± 263**	197 ± 39	247 ± 96	**442 ± 88**
Ethyne	**4981 ± 627**	**2023 ± 985**	286 ± 239	103 ± 21	236 ± 55	331 ± 66
Ethane	**3585** ± 1018	**1655 ± 366**	**1686 ± 1514**	866 ± 173	**2978 ± 1473**	771 ± 154
Propene	**5119 ± 758**	**1588 ± 448**	251 ± 64	187 ± 37	228 ± 55	256 ± 51
Propane	**4723 ± 3622**	**1533 ± 779**	**825 ± 613**	504 ± 101	**1007 ± 476**	257 ± 51
Propyne	**681 ± 38**	**351 ± 182**	73 ± 28	b.d.	66 ± 19	b.d.
Acetaldehyde	**3067 ± 2355**	**591 ± 181**	**336 ± 139**	91 ± 18	**382 ± 112**	b.d.
2-Methylpropane	**2666 ± 1878**	**660 ± 542**	**504 ± 441**	70 ± 14	**255 ± 134**	77 ± 15
Methanol	**7275 ± 4012**	**6631 ± 2646**	**4996 ± 3082**	**4192 ± 838**	2608 ± 612	2564 ± 513
1-Butene/ i-butene	**2482 ± 304**	**740 ± 297**	**300 ± 412**	100 ± 20	111 ± 21	**156 ± 31**
1,3-Butadiene	**731 ± 73**	**249 ± 109**	43 ± 11	b.d.	26 ± 15	b.d.
n-Butane	**6140 ± 3760**	**1626 ± 938**	b.d.	555 ± 111	623 ± 676	220 ± 44
trans-2-Butene	**814 ± 314**	**123 ± 30**	16 ± 3	**61 ± 12**	25 ± 10	10 ± 2
cis-2-Butene	**784 ± 301**	**130 ± 39**	**74 ± 38**	24 ± 5	21 ± 12	**81 ± 16**
1,2-Butadiene	**181 ± 181**	b.d.	**33 ± 7**	b.d.	b.d.	b.d.
Ethanol	**17 622 ± 8707**	**10 462 ± 7825**	333 ± 189	229 ± 46	312 ± 93	113 ± 23
3-Methyl-1-butene	**224 ± 112**	**99 ± 37**	52 ± 6	b.d.	16 ± 33	b.d.
2-Methylbutane	**30 906 ± 10 821**	**3913 ± 1668**	465 ± 178	b.d.	306 ± 90	**656 ± 131**
Acetone	**12 328 ± 7453**	**6827 ± 5420**	**10 721 ± 24 004**	**37 040 ± 7408**	3798 ± 1856	2703 ± 541
1-Pentene	**605 ± 220**	**86 ± 39**	35 ± 8	b.d.	29 ± 16	26 ± 5
2-Propanol	**612 ± 612**	**420 ± 357**	44 ± 14	b.d.	42 ± 17	**81 ± 16**
2-Methyl-1-butene	**1014 ± 173**	**71 ± 108**	b.d.	b.d.	b.d.	b.d.
n-Pentane	**7886 ± 2785**	**1121 ± 521**	242 ± 106	57 ± 11	165 ± 52	241 ± 48
Isoprene	b.d.	157 ± 93	266 ± 159	1414 ± 283	1320 ± 363	776 ± 155
trans-2-Pentene	**1421 ± 173**	**214 ± 91**	**28 ± 13**	b.d.	b.d.	14 ± 3
cis-2-Pentene	**959 ± 270**	**161 ± 50**	22 ± 9	15 ± 3	b.d.	11 ± 2
Propanal	**1251 ± 1251**	**737 ± 1120**	54 ± 24	b.d.	58 ± 79	76 ± 15
2-Methyl-2-butene	**40 ± 40**	**36 ± 66**	11 ± 8	b.d.	b.d.	b.d.
Acetic acid menthyl ester	b.d.	b.d.	b.d.	b.d.	b.d.	b.d.
1,3-Pentadiene	b.d.	**47 ± 117**	14 ± 4	b.d.	b.d.	b.d.
Cyclopentadiene	b.d.	b.d.	35 ± 14	b.d.	45 ± 22	b.d.
2,2-Dimethylbutane	**6385 ± 1992**	**875 ± 364**	117 ± 111	67 ± 13	112 ± 110	**175 ± 35**
2-Butanol	b.d.	**3103 ± 8097**	**117 ± 156**	b.d.	59 ± 23	102 ± 20
1-Propanol	**502 ± 502**	**418 ± 259**	**342 ± 377**	94 ± 19	b.d.	b.d.
Cyclopentene	**335 ± 335**	**27 ± 75**	**39 ± 11**	b.d.	b.d.	b.d.
Methacrolein	b.d.	b.d.	80 ± 37	287 ± 57	147 ± 49	200 ± 40
Cyclopentane/2,3-dimethylbutane	**2646 ± 792**	**6075 ± 15 604**	**275 ± 316**	**277 ± 55**	88 ± 27	139 ± 28
2-Methylpentane	**4772 ± 2172**	**1274 ± 500**	232 ± 112	45 ± 9	160 ± 100	**291 ± 58**
Methyl vinyl ketone	b.d.	b.d.	102±	389 ± 78	171 ± 38	194 ± 39
Butanal	**1319 ± 877**	253 ± 190	133 ± 56	b.d.	126 ± 99	b.d.
1-Hexene	**47 ± 47**	20 ± 58	**113 ± 68**	**129 ± 26**	40 ± 54	38 ± 8
3-Methylpentane	**2259 ± 557**	**572 ± 250**	**73 ± 40**	42 ± 8	54 ± 19	**123 ± 25**
2-Methyl-1-pentene	**243 ± 85**	**54 ± 55**	14 ± 3	b.d.	b.d.	b.d.
n-Hexane	**1848 ± 516**	**484 ± 204**	**127 ± 99**	80 ± 16	95 ± 58	60 ± 12
trans-2-Hexene	**190 ± 46**	**59 ± 21**	**110 ± 53**	15 ± 3	**26 ± 14**	11 ± 2
cis-2-Hexene	**111 ± 38**	**65 ± 41**	**107 ± 21**	11 ± 2	b.d.	b.d.
1,3-Hexadiene (trans)	**85 ± 85**	27 ± 52	**53 ± 10**	34 ± 7	b.d.	b.d.
Methylcyclopentane	b.d.	**36 ± 103**	**49 ± 13**	22 ± 4	b.d.	b.d.
2,4-Dimethylpentane	**1490 ± 410**	**361 ± 180**	54 ± 28	14 ± 3	43 ± 14	**111 ± 22**
Methylcyclopentene	**333 ± 79**	**54 ± 98**	14 ± 5	b.d.	b.d.	b.d.
Benzene	**2281 ± 796**	**1383 ± 349**	**303 ± 238**	155 ± 31	199 ± 35	224 ± 45
1-Butanol	b.d.	**145 ± 359**	28 ± 14	b.d.	39 ± 19	b.d.
Cyclohexane	**743 ± 213**	**198 ± 77**	39 ± 23	18 ± 4	33 ± 14	**46 ± 9**
2-Methylhexane	**708 ± 132**	**256 ± 144**	36 ± 14	23 ± 5	34 ± 24	35 ± 7
2,3-Dimethylpentane	**684 ± 300**	**114 ± 41**	23 ± 14	**36 ± 7**	17 ± 16	18 ± 4

Table 8. Continued.

Compound	Locations dominated by engine-related emissions		Urban background	Locations dominated by biogenic emissions		
	Motorway, traffic jam 2 samples	Tiergarten tunnel 10 samples	Nansenstrasse 14 samples	Pfaueninsel 1 sample	Treptower Park 11 samples	Grunewald 1 sample
3-Methylhexane	**894 ± 138**	**268 ± 84**	82 ± 34	54 ± 11	109 ± 33	110 ± 22
Pentanal	**102 ± 14**	12 ± 22	11 ± 2	b.d.	b.d.	b.d.
Cyclohexene	b.d.	b.d.	18 ± 4	b.d.	b.d.	b.d.
1,3-Dimethylcyclopentane (cis)	**287 ± 2**	**74 ± 40**	11 ± 5	11 ± 2	b.d.	19 ± 4
1-Heptene	**138 ± 42**	25 ± 31	17 ± 10	b.d.	b.d.	13 ± 3
2,2,4-Trimethylpentane	**545 ± 10**	**188 ± 55**	28 ± 15	b.d.	24 ± 10	34 ± 7
Heptane	**467 ± 35**	**146 ± 71**	32 ± 11	18 ± 4	29 ± 9	37 ± 7
2,3-Dimethyl-2-pentene	b.d.	27 ± 61	b.d.	b.d.	b.d.	b.d.
Octene	28 ± 28	b.d.	b.d.	b.d.	b.d.	b.d.
Methylcyclohexane	**146 ± 78**	**122 ± 46**	27 ± 15	b.d.	18 ± 15	14 ± 3
2,3,4-Trimethylpentane	**327 ± 73**	**120 ± 46**	20 ± 14	24 ± 5	19 ± 5	10 ± 2
Toluene	**8553 ± 1675**	**2679 ± 1012**	**407 ± 237**	299 ± 60	276 ± 133	212 ± 42
2-Methylheptane	**253 ± 110**	**114 ± 63**	25 ± 17	b.d.	17 ± 12	10 ± 2
4-Methylheptane	**254 ± 110**	**85 ± 43**	14 ± 9	b.d.	11 ± 10	b.d.
3-Methylheptane	**121 + 67**	**82 ± 45**	17 ± 13	68 ± 14	b.d.	26 ± 5
Hexanal	108 ± 108	**52 ± 86**	**72 ± 46**	b.d.	**129 ± 69**	12 ± 2
Acetic acid butyl ester	b.d.	b.d.	b.d.	b.d.	b.d.	b.d.
n-Octane	**208 ± 45**	**107 ± 93**	28 ± 23	23 ± 5	24 ± 11	**34 ± 7**
Dimethylcyclohexane isomer	b.d.	b.d.	b.d.	b.d.	b.d.	b.d.
Ethylbenzene	**1285 ± 200**	**485 ± 207**	76 ± 40	21 ± 4	55 ± 31	**127 ± 25**
m/p-Xylene	**3301 ± 568**	**1853 ± 2411**	151 ± 97	31 ± 6	109 ± 68	**263 ± 53**
Heptanal	b,d.	b.d.	22 ± 14	b.d.	93 ± 62	b.d.
Styrene	**277 ± 67**	**117 ± 21**	57 ± 40	b.d.	41 ± 7	35 ± 7
1-Nonene	b.d.	b.d.	b.d.	b.d.	b.d.	b.d.
o-Xylene	**1344 ± 150**	**408 ± 149**	64 ± 38	13 ± 3	49 ± 28	**106 ± 21**
n-Nonane	**221 ± 65**	**91 ± 22**	21 ± 4	12 ± 2	20 ± 6	19 ± 4
i-Propylbenzene	**92 ± 36**	**50 ± 15**	**30 ± 70**	15 ± 3	11 ± 8	b.d.
α-Pinene	b.d.	b.d.	31 ± 26	30 ± 6	176 ± 370	81 ± 16
n-Propylbenzene	**271 ± 48**	94 ± 43	20 ± 13	66 ± 13	12 ± 6	88 ± 18
m-Ethyltoluene	**832 ± 136**	**214 ± 131**	31 ± 26	b.d.	25 ± 15	**63 ± 13**
p-Ethyltoluene	**331 ± 37**	**201 ± 85**	24 ± 14	b.d.	18 ± 8	20 ± 4
1,3,5-Trimethylbenzene (1,3,5-TMB)	**278 ± 77**	**210 ± 122**	**46 ± 55**	41 ± 8	35 ± 32	45 ± 9
Sabinene	b.d.	b.d.	b.d.	b.d.	b.d.	b.d.
o-Ethyltoluene	**336 ± 45**	**159 ± 64**	36 ± 24	b.d.	**67 ± 30**	30 ± 6
Octanal	b.d.	b.d.	13 ± 5	b.d.	b.d.	b.d.
β-Pinene	b.d.	b.d.	15 ± 8	b.d.	18 ± 10	36 ± 7
1,2,4-Trimethylbenzene/t-butylbenzene	**1514 + 292**	**462 ± 127**	**63 ± 37**	**172 ± 34**	43 ± 19	45 ± 9
n-Decane	**305 ± 159**	**92 ± 49**	22 ± 8	**101 ± 20**	17 ± 9	29 ± 6
1,2,3-Trimethylbenzene (1,2,3-TMB)	**632 ± 350**	**108 ± 51**	**120 ± 296**	**511 ± 102**	27 ± 20	49 ± 10
Limonene	b.d.	b.d.	b.d.	b.d.	b.d.	b.d.
Eucalyptol	b.d.	b.d.	b.d.	57 ± 11	b.d.	24 ± 5
Indane	71 ± 71	b.d.	b.d.	49 ± 10	b.d.	b.d.
1,3-Diethylbenzene	**187 ± 6**	**57 ± 40**	13 ± 11	b.d.	b.d.	17 ± 3
1,4-Diethylbenzene	**252 ± 71**	**52 ± 34**	**522 ± 1380**	b.d.	b.d.	11 ± 2
Butylbenzene	**232 ± 70**	**60 ± 34**	b.d.l.	b.d.	b.d.	b.d.
n-Undecane	**45 ± 7**	16 ± 6	10 ± 13	b.d.	22 ± 10	b.d.
n-Dodecane	24 ± 13	b.d.	26 ± 24	b.d.	b.d.	b.d.
n-Tridecane	b.d.	b.d.	b.d.	b.d.	b.d.	10 ± 2

to evaluate exacerbating or improving effects of vegetation (part (2), see overview in Table 9). All traffic-related pollutants (CO and NO_x, PNC and different PM) display similar features. The highest absolute and relative CO median level was identified in traffic-related areas, declining towards urban green spaces and residential areas. With respect to residential areas, the ventilation (continuous and discontinuous buildings) was identified as an important factor. The lowest levels were detected at forests and agricultural areas. Regarding NO_x, median relative values during summertime were 15.1 for NO and 1.3 for NO_2 for all measurements, i.e., notably enhanced with respect to the reference site, whereas the median of the relative values for NO and NO_2 were 23.9 and 19.2 for residential areas classified as urban (continuous and discontinuous buildings) and 15.7 and 12.2 in commercial areas and transport, respectively (Fig. 8). It is well known that substantial amounts of NO_2 are produced and released by oxidation in catalytic converters of diesel cars (Li et al., 2007). Of the passenger car fleet of Berlin, 29.9 ± 3.5 % cars are diesel; of the light-duty commercial vehicles 93.1 ± 0.7 %

Table 9. Effect of different vegetated areas on the median amount of atmospheric pollutants ±5 % quantiles and their change in Berlin during BAERLIN2014. Bold numbers of changes represent statistical significance by 95 %. Gaseous pollutants are listed at the top and particulate values based on bicycle observations at the bottom.

Land surface type	CO (ng)		NO_x		O_3		Ox	
	ppb_v	change, %	ppb_v	change, %	ppb_v	change, %	ppb_v	change, %
Urban background, Neukölln	201.0 ± 4.5	–	11.2 ± 1.4	–	29.0 ± 1.8	–	40.4 ± 1.4	–
Green spaces	143.7 ± 3.4	$\mathbf{-30.3 \pm 3.0}$	58.1 ± 14.2	$\mathbf{+274.2 \pm 108.1}$	20.0 ± 1.5	$\mathbf{-41.5 \pm 3.8}$	54.2 ± 3.8	$+0.4 \pm 8.1$
Forests	126.6 ± 3.5	$\mathbf{-34.9 \pm 4.3}$	14.7 ± 3.5	0.5 ± 26.8	24.7 ± 2.2	$\mathbf{-32.7 \pm 3.2}$	43.4 ± 3.0	$\mathbf{-24.6 \pm 5.4}$
deciduous	130.0 ± 2.2	$\mathbf{-34.8 \pm 4.4}$	15.4 ± 3.8	-0.4 ± 24.9	25.7 ± 2.0	$\mathbf{-31.2 \pm 3.1}$	43.4 ± 2.8	$\mathbf{-25.7 \pm 5.2}$
coniferous	120.5 ± 2.9	$\mathbf{-34.7 \pm 4.8}$	13.8 ± 2.5	-6.2 ± 22.8	22.7 ± 1.9	$\mathbf{-35.9 \pm 3.5}$	42.4 ± 2.0	$\mathbf{-18 \pm 5.3}$
mixed	131.1 ± 1.8	$\mathbf{-35.5 \pm 2.2}$	21.3 ± 7.1	$\mathbf{+73.7 \pm 56.9}$	27.3 ± 2.4	$\mathbf{-27.2 \pm 3.9}$	52.3 ± 5.2	$\mathbf{-8.6 \pm 5.8}$
Agricultural areas	127.4 ± 1.1	$\mathbf{-34.0 \pm 1.6}$	8.7 ± 2.3	-0.1 ± 26.6	37.8 ± 1.2	$\mathbf{-13.2 \pm 1.9}$	49.5 ± 1.5	$\mathbf{-9.8 \pm 1.7}$
Land surface type	PNC		PM_1		PM_{10}			
	ppb_v	change (%)	$\mu g\,m^{-3}$	change (%)	$\mu g\,m^{-3}$	change (%)		
Urban background, Neukölln	7711 ± 188	–	5.5 ± 0.6	–	16.0 ± 0.9	–		
Green spaces	7270 ± 501	$\mathbf{-16.7 \pm 10.9}$	3.6 ± 0.2	$\mathbf{-37.2 \pm 2.9}$	9.9 ± 0.9	$\mathbf{-46.9 \pm 5.8}$		
Forests	5468 ± 536	$\mathbf{-35.2 \pm 4.6}$	2.1 ± 0.1	$\mathbf{-47.4 \pm 4.7}$	6.7 ± 0.8	$\mathbf{-58.8 \pm 4.9}$		
deciduous	4991 ± 419	$\mathbf{-38.6 \pm 2.6}$	2.0 ± 0.1	$\mathbf{-53.2 \pm 6.0}$	5.9 ± 0.6	$\mathbf{-63.6 \pm 4.2}$		
coniferous	5802 ± 657	$\mathbf{-31.6 \pm 6.0}$	2.1 ± 0.1	$\mathbf{-47.0 \pm 5.4}$	7.1 ± 0.9	$\mathbf{-56.8 \pm 4.7}$		
mixed	6059 ± 564	$\mathbf{-26.6 \pm 6.7}$	2.3 ± 0.1	$\mathbf{-40.6 \pm 2.6}$	7.8 ± 1.3	$\mathbf{49.7 \pm 5.0}$		

are diesel (Berlin Senate, personal communication). Based on the study of Tullius and Lutz (2003) it is expected that this source type contributes significantly (33 %) to the measured nitrogen oxides mixing ratios, especially in urban areas with notable traffic and transport. Other sources like the energy industries, non-energy combustion, non-road transportation and industry provide the remaining 67 % of NO_x production, excluding ship emissions for which Tullius and Lutz (2003) did not have information. However, a detailed calculation of the NO_x budget was out of the scope of this campaign. Therefore we can state that for most of the road-related area analyzed the mixing ratios were found to be higher than in Neukölln, except the extensive background sites such as forest or remote agricultural areas outside of Berlin. Near green spaces like parks, NO_x was found at its highest level.

The observed volume mixing ratios of ozone are a product of photolysis rates, NO_x and VOCs described above. In this way the urban ozone mixing ratio is closely related to the mixing ratios of NO and NO_2, as well as the photolysis rate of NO_2. To account for this cycling of NO_x and ozone we consider a photostationary steady state. The emitted NO reacts with ambient ozone to be converted into NO_2. The NO_2 can subsequently be rapidly photolyzed back to NO and $O(^3P)$, which subsequently reforms ozone, in the case of sufficiently strong solar radiation. Through these reactions, ozone is rapidly consumed by reaction with NO, if NO is present in substantial amounts, and re-formed by the subsequent photolysis of NO_2. In a remote or background location, with no additional sources of NO_2, the relative mixing ratios of NO, NO_2 and ozone are determined by the photolysis rate of NO_2. In order to capture such a linkage we introduce the sum of ozone and NO_2 as Ox. In this way the ozone–NO_x conversion cycle is considered.

Median values for urban residential areas were situated around 28 ppb_v for ozone and 52 ppb_v for Ox. The highest median ozone values were found in agricultural areas 46.5 ppb_v and the lowest in the vicinity of parks 17 ppb_v corresponding to the detected high levels of NO_x. While urban Ox levels were found rather uniform significantly enhanced only in traffic-influenced areas (+30 % because of NO_x emission), much lower Ox mixing ratios were observed for agricultural areas (−10 %) and within forests (−25 %), with the exact values depending on the forest tree type (Fig. 9). Thus, locations near the category green spaces have only moderate dampening effects on ozone mainly due to the NO and NO_2 present. NO_x should first be addressed because it causes significant changes in O_3.

As done in the case of the gaseous parameters, the observations were classified by the land use type based on the CORINE land cover (number: Fig. S3.1.1, mass: Fig. 10). Again, there were clear effects from ventilation: urban areas with block buildings (continuous buildings) showed a slightly enhanced particle level compared to areas with single houses (discontinuous buildings). This is supported by an increase in concentration with decreasing street canyon width: compare, for example, bicycle tracks starting at Fehrbelliner Platz (widest) along Hohenzollerndamm via Lietzenburger Straße (+26 % in PNC compared to Fehrbelliner Platz) until Urania (denser; +96 % in PNC compared to Fehrbelliner Platz). In addition, the relative enhancement in particle number concentrations at Urania was largest along the exemplary track. PNCs were found to be highest in industrial and commercial areas with notable transport and production of goods (e.g., Kurfürstendamm, Kantstraße, Greifswalder Straße and Frankfurter Allee): $+47 \pm 11$ % for baseline concentrations and $+63 \pm 10$ % for all the observations (van) compared to

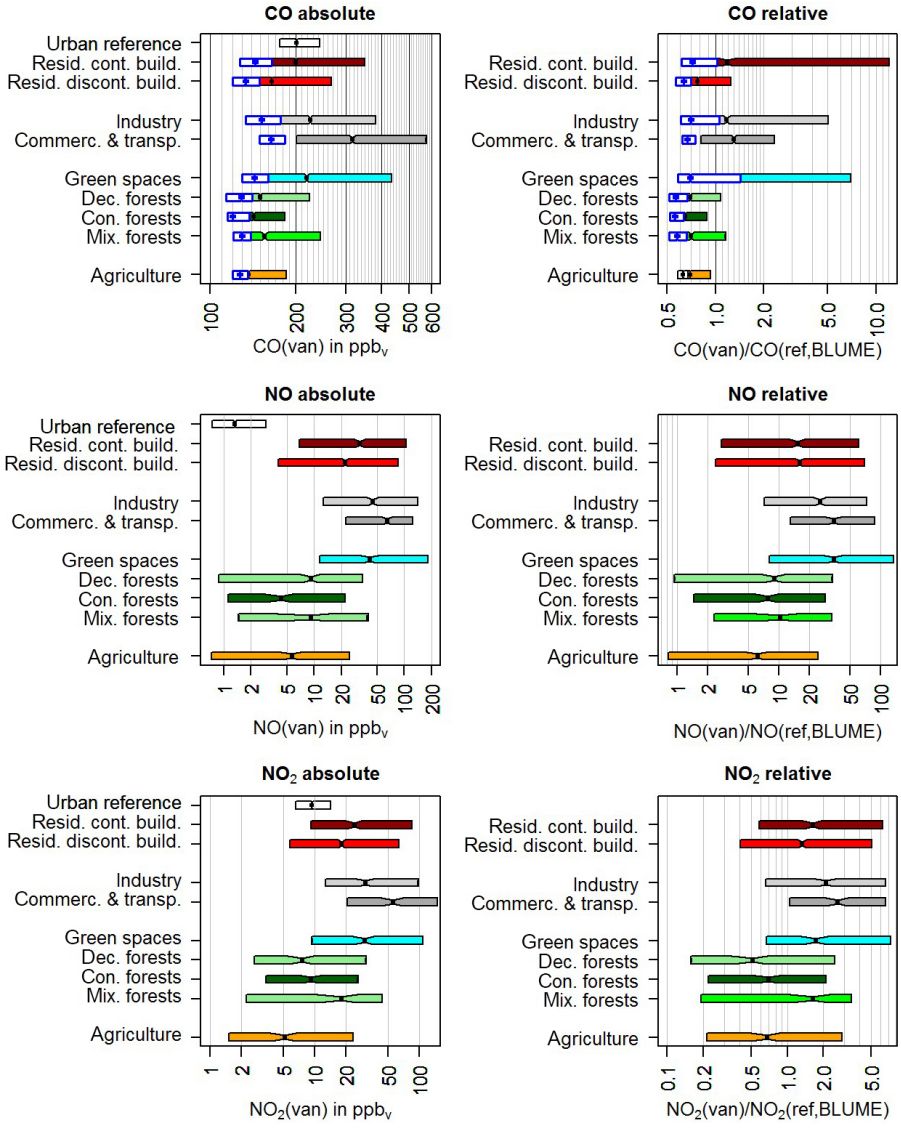

Figure 8. Box plots of CO, NO and NO_2 mobile measurement values (left graphs) and ratios of mobile measurements relative to Neukölln (right graphs) in areas of different land use (CORINE). The box plots start and end at the 25th and 75th percentile with a notch between the 45th and 55th percentiles. Blue outlined transparent bars in the CO graphs refer to the so-called baseline values, while the colored bars represent all the observations. Shaded bars indicate an insufficient number of data points. Values and number of corresponding values are given in the supporting online information (SOI).

the reference site in Neukölln. The variation in PNC_{10} can be clearly seen on one of the standard bicycle tracks from Potsdam cycling through the forest of Grunewald before entering the city center of Berlin in Charlottenburg from the west along major traffic routes (Fig. 11). A clear effect of green spaces and forests on PNC is visible: urban green spaces (parks and vegetated leisure areas) resulted in a reduction by 15 ± 7 %, which was only seen for bicycle measurements as the van was unable to enter, and so just passed, those areas. Due to the course resolution of CORINE (Bossard et al., 2000) the van measurements in the vicinity were classified as green spaces too and, therefore, median values of bicycle and van-based measurements differed substantially. In this case we found the bicycle measurements to be more representative reliable results. For forests, similar but more intense number effects were visible (bicycle: -33 ± 4 %; van: -28 to -34 %). It can be concluded that in vegetated areas PNC declines remarkably.

The situation was less clear for particulate masses; e.g., for PM_{10} the changes depended on the platform. The PM_{10} measurements by van indicated a rather identical picture at street level, while the bicycle-based measurements showed a remarkable decline for green spaces (-45 ± 8 %) and forests (> -50 %). In contrast, $relPM_{10}$ increased in industrial, com-

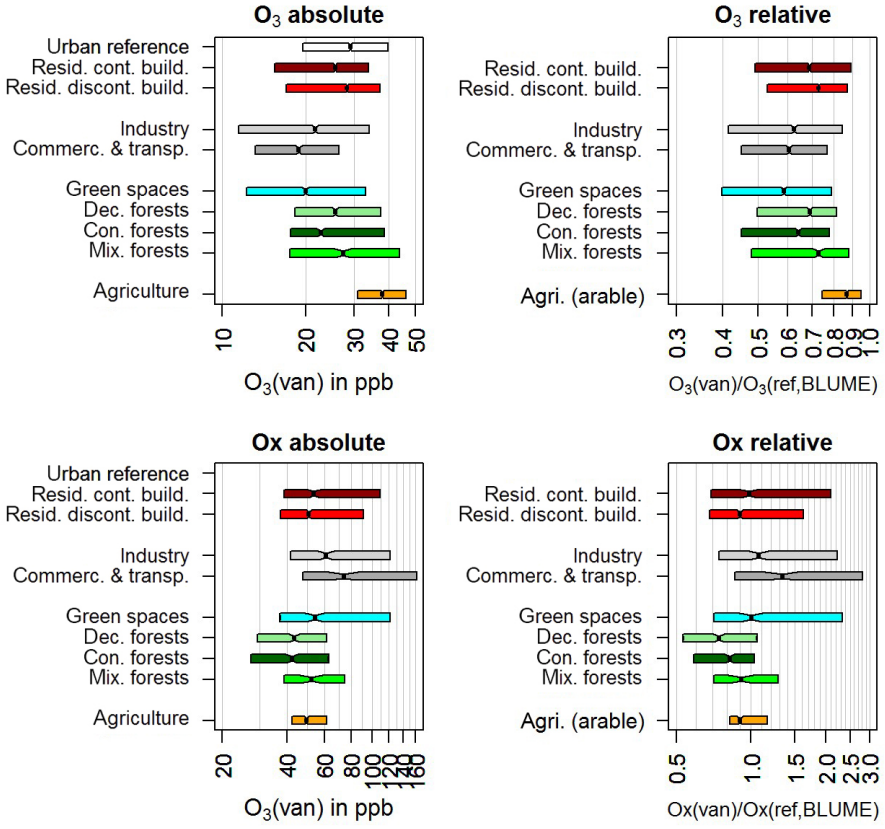

Figure 9. Box plots of mobile measurements (left) and relative (right) values box plots for ozone (top) and Ox (bottom) with respect to different surface type usage based on CORINE. Box plots range from the 25th to the 75th percentile each with notches from the 45th to the 55th percentile centered around the median. Shaded bars indicate an insufficient number of data points. Values and the corresponding numbers of available data are provided in SOI.

mercial and transport-affected areas by $+44 \pm 9$ to a remarkable extent. Thus we can conclude that vegetation-affected surface areas substantially reduced the burden of particulate mass and particle number as displayed by the bicycle measurements. Differences between the bicycle and van platform data likely stem from the circumstance that different tracks had to be used and the coarse CORINE classification sometimes treated even major roads next to a park as park surface. Initial analyses of individual bicycle videos have indicated primarily traffic-related sources for occurrences of high concentrations of particles, such as old double decker busses, mopeds and single ships when crossing bridges. Detailed results from this investigation will be published elsewhere.

5 Conclusions

The mobile measurements with bicycle, van and air plane/glider as part of the BAERLIN2014 measurement campaign have demonstrated the ability of integrated measurement platforms to characterize air quality on multiple scales, i.e., from meter to regional resolution. Van-based measurements were used to cover a large geographical area in and around the city of Berlin, while bicycles covered a range of main streets but also penetrated to areas inaccessible for cars (pedestrian areas, parks and forested areas). Bicycles were found to be a cheap, flexible and reliable platform for characterizing the spatiotemporal variations in pollutant concentrations and meteorological conditions over the 3-month campaign period. Two benefits of combining bicycle and van measurements were found: (1) the different speed at usual conditions and thus an improved horizontal resolution and higher local variation of data with respect to particle number concentration of bicycle measurements at identical time resolution and potential parallel observations at identical time at different distance to the particle source; and (2) the impact of the particle lifetime on the agreement of number (relevant for smaller sizes) and mass (relevant for larger sizes) concentrations observed by the two platforms. With respect to (point 1) the exhaust of, for instance, a car gathering speed and therefore contributing to new particle formation was found to enhance the $PNC_{2.5}$ of the van in a more intense way than for PNC_{10} for bicycles, while hardly any change between both

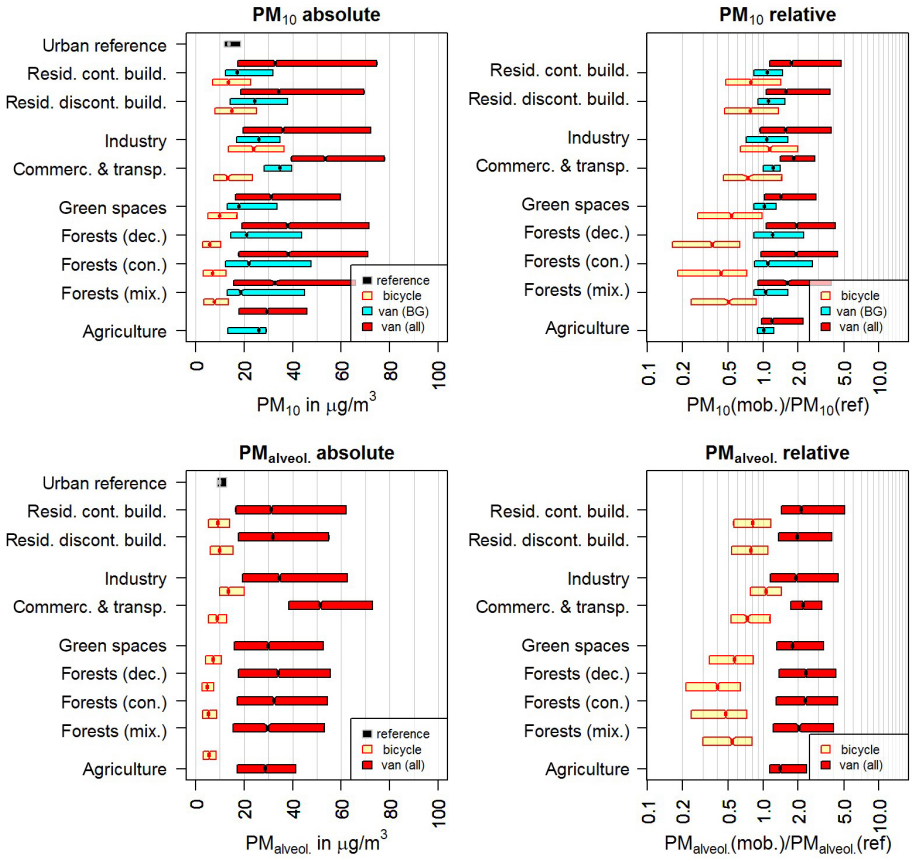

Figure 10. Particulate mass concentrations (left) and concentration ratios (right) for different land surface types and different observation platforms compared to the measurements in Neukölln: top – PM_{10}, bottom – PM(alveolar).

platforms was seen with respect to the mass (point 2) as found in other studies too (Birmili et al., 2013). Comparison of van and bicycle measurements (particulate properties and temperature only) agreed within the uncertainty level under identical measurement conditions. The relative value approach used for individual parameters to compare different measurements of trace gases and aerosol particles by different platforms in different conditions was found to be very applicable for the studies aims.

Hotspots of elevated air pollutant concentrations in Berlin were identified and indicated traffic to be most likely the major origin. This was supported by airplane measurements, which displayed moderate regional concentrations, increased by emissions from Berlin, plus substantially elevated particle number concentrations in air masses from both coal-fired power plants and within the flight corridor of Tegel airport. As a consequence, emissions within the urban area of Berlin were responsible for the elevated particle levels between June and August 2014. Canister samples displayed the presence of remarkably elevated AVOCs between 19 times and 50 times higher values than the corresponding values at the reference site (urban background). These observations are in good agreement with other studies (e.g., von der Weiden-Reinmüller et al., 2014).

A significant influence of vegetation on pollutant concentrations was also observed with quite substantial concentrations of BVOCs, such as isoprene and monoterpenes. Differences in effects were noted between three broadly different types of vegetation: agricultural areas, urban green spaces and urban forests. While agricultural areas showed similar particle number and mass concentrations relative to the urban background, significantly reduced particle concentrations (number and mass) were observed in both forests and parks, indicating a reduced production of and/or a substantial sink for particles. Therefore vegetation can be assumed as substantial reduction tool for urban particle levels and partially for trace gases.

However, the trace gas effect was dependent on vegetation area size and composition. Urban green spaces (e.g., parks) with much smaller sizes than urban forested areas were shown to have not significantly lower but rather elevated NO or NO_2 concentrations than the urban background station in Neukölln. This is in contrast to both agricultural areas and urban forests, which showed significantly lower mixing ratios of NO_2 compared to the urban background.

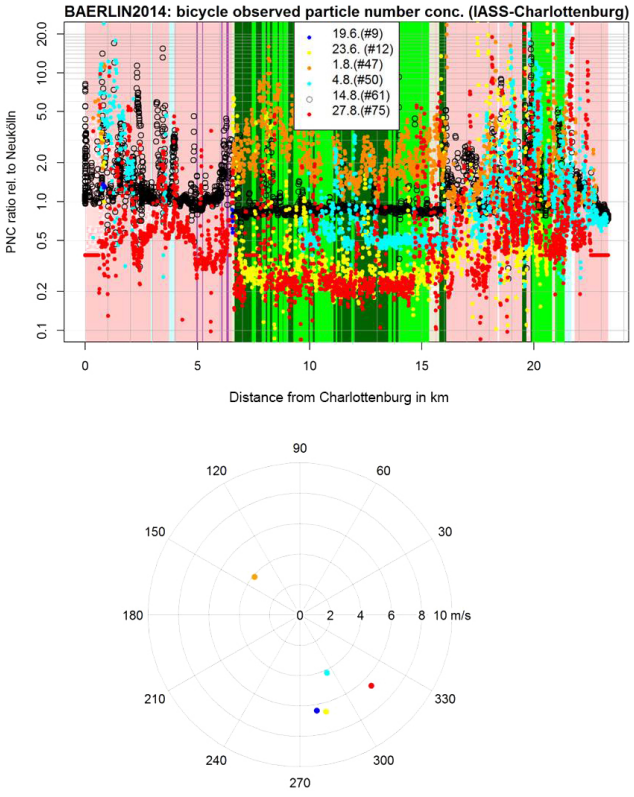

Figure 11. Top: measurements by bicycle, following the same route, Charlottenburg (Berlin) to IASS (Potsdam), on different days and during different times. The dots plotted are particle number concentration ratios relative to the stationary site in Neukölln with a time resolution of 10 s. Green shaded areas are vegetated areas; pink shaded areas are anthropogenically dominated areas. Bottom: wind rose and speed at Tempelhof (DWD) measured for the times of the individual tracks. The color coding is identical with that in the upper graph. Note that the corresponding wind data for track 61 are not available.

The ozone production cycle marker Ox was substantially reduced in urban forests, causing a lower ozone production and a corresponding increased lifetime of VOCs. As both NO_2 and Ox decreased substantially towards forests, a photostationary steady state cannot be assumed for the entire area of Berlin but rather only for residential areas, industrial, commercial and transport-affected areas and green spaces (e.g., parks). Our results suggest that increased urban green spaces and forested areas would be a viable method to reduce particulate pollution if substantial in dimension, but not necessarily for ozone or NO_2. Reduction of NO mixing ratios would require reduction in emissions from traffic, which would be expected to lead to an increase in the mixing ratio of ozone. The intensity of this increase would be dependent on the biogenic feedback processes involving the emission on BVOCs and the formation of secondary organic aerosol mass.

The new approach using bicycles in addition to van measurements for a detailed microscale investigation yielded important additional information for areas not accessible for road-based mobile platforms such as vans and for regions most relevant for pedestrians and cyclists. For instance, particle number concentrations varied by orders of magnitude when shifting from the center of the road to the walkway and when approaching bus stops or traffic lights from the pedestrian point of view. A further development of miniature observation instruments for other pollutants such as nitrogen oxides, CO and BC would be highly recommended to address not only the street center but also the area most relevant for the health of local citizens. The BAERLIN2014 campaign was conducted for summertime conditions (June to August 2014) in a selected region representing various environments present in of the area investigated. Clearly planned annual observations of different urban conditions (in different environments) by a multitude of cheap bicycle observation methods, making use of volunteers cyclists, would improve the basis for an observation-based pollution map of the city. We underline the importance of an improved resolution and updated surface coverage map (compared to the current CORINE land cover) with more surface information such as vegetation type, streets or buildings for any stratification approach based on surface types.

To explore the effects and sensitivities of different vegetated land cover types, we recommend investigating the data further with detailed atmosphere–biosphere chemistry-transport models and box model simulations, which can then be used to test mitigation scenarios.

6 Data availability

This study is one of two overview articles about the BAERLIN2014 campaign. The corresponding dataset will be made available for everyone during the next months, when the second part (von Schneidemesser et al., 2016) about the stationary measurements and the source apportionment is published.

Appendix A: Information on instrument and methods applied

Table A1. List of applied instruments, time resolutions, uncertainties and detection limits/ranges.

Meas. platform (resp. inst.)	Parameter	Instrument	Time resolution	Uncertainty	Detection limit or range
Bicycle (IASS)	PNC, mod. mean size, lung deposited surface area	DiSCmini, Matter Aerosol (Wohlen, CH)	1 s	15 % (500 cm^{-3}), 30%, 15 %	10^3–10^6 cm^{-3} μm^2 cm^{-3} (D_p: 10–500 nm)
Bicycle (IASS)	PM_{10}, $PM_{2.5}$, PM_1, PM_{health}, PSD, MSD	model 1.108, GRIMM (Ainring, D)	6 s	3 % 3 %	0.1–10^5 $\mu g\ m^{-3}$ 1–2 × 10^6 cm^{-3} (D_p: 0.3–20 µm)
Bicycle (IASS)	temperature and RH	model 1.154, GRIMM (Ainring, D)	12 s	±0.1 °C/1 % RH	0–80 °C/10–95 %
Bicycle (IASS)	GPS position and video	Garmin Virb Elite HD action camera	1 s	between 2 and 5 m depending on speed	< 8 h depending on resolution
Van (RC Jülich)	particle number	ELPI, Dekati (Kangasala, FI)	1 s	10 %	0.1–10^7 cm^{-3} (f(size)) (D_p: 0.007–10 µm)
Van (RC Jülich)	particle number	NanoCPC 3788, TSI (Aachen, D)	1 s	10 %	0–4 × 10^5 cm^{-3} (D_p: 0.003–3 µm)
Van (RC Jülich)	NO, NO_2, O_3	CLD 770, Chemiluminescence	5 s	5 % (NO&NO_2), 10 % (O_3)	40 ppt (NO&O_3) 80 ppt (NO_2)
Van (RC Jülich)	CO	UV–resonance–fluorescence	1 s	1.3 ppb_v	1 ppb_v
Van (RC Jülich)	CO_2, CH_4	cavity ring-down spectrometer	0.1 s	≤ 200 ppb_v, (CO_2) ≤ 3 ppb_v (CH_4)	≈ 200 ppb_v, (CO_2) ≈ 3 ppb_v (CH_4)
Van (RC Jülich)	temperature and RH	HMT 330, Vaisala (Helsinki, FI)	1 s	0.2 °C 1 % RH	−60 to +160 °C 0–100 %
Van (RC Jülich)	wind direction & speed	WMT 50 Vaisala (Helsinki, FI)	1 s	5 %	0–60 $m\ s^{-1}$
Van (RC Jülich)	Position	WBT202, Wintec (Milpitas, USA)	1 s	±5 m	–
Ultralight (KIT)	T, dew point	TP3-S, Meteolabor (Baiersdorf, D)	1 s	±0.25 K ±0.25 K	−30 to +50 °C −80 to +60 °C
Ultralight (KIT)	N_{total} (D_p > 4.5 nm)	5.410 SKY OPC, GRIMM (Ainring, D)	1 s	10 %	0.1–10^7 cm^{-3}
Ultralight (KIT)	PSD: low. sizes, 4.5–350 nm upp. sizes, 0.3–20 µm, PM	SMPS 5.403, GRIMM (Ainring, D) OPC 1.108, GRIMM (Ainring, D)	2 min	3–15 % (f(size)) 3 %	0.1–10^7 cm^{-3} 0.1–10^5 $\mu g\ m^{-3}$
Ultralight (KIT)	soot/BC	AE33 AVIO, AEROSOL d.o.o., (Ljubljana, SLO)	1 min	10 %	0.03–100 $\mu g\ m^{-3}$ (1 min), 5 L min^{-1}
DA42 (HSD)	T, RH	Voltcraft, DL-121 TH	2 s	1 °C, 3 % RH	−40 to (+70) °C
DA42 (HSD)	UF-N_{total} (D_p: 25–300 nm)	NanoCheck 1320, GRIMM (Ainring, D)	10 s	30 %	5 × 10^2–5 × 10^5 cm^{-3}
DA42 (HSD)	PSD (0.25–32 µm), PM	1.109, Grimm (Ainring, D)	6 s	3 %	1–10^6 cm^{-3}
DA42 (HSD)	soot/BC	AE 33 Avio, Magee, Ljubliana, SLO	1 s	10 %	0.03–100 $\mu g\ m^{-3}$ (1 min), 5 L min^{-1}
DA42 (HSD)	SO_2	APSA-370, Horiba	15 s	1 %	pm

Information about the Supplement

Further tables and graphs on frequency distributions of gases and particle properties are available in the Supplement.

The Supplement related to this article is available online at doi:10.5194/acp-16-7785-2016-supplement.

Acknowledgements. The authors thank all the cyclists at the institute for their high motivation and enthusiasm even during poor weather conditions. We are very grateful to Aerosol d.o.o. Slovenia for supplying the MAGEE AE 33 Avio for the airborne DA 42 studies. Thanks go to Alfred Wiedensohler, Wolfram Birmili, Kay Weinhold and colleagues for calibration of the particle instruments and further support regarding the measurements. We thank numerous colleagues at the IASS in Potsdam who provided various types of support. Without them the present study would not have been possible. The same gratitude applies to the colleagues at the Leibnitz institute for tropospheric research in Leipzig (Germany) for continuing support and discussion.

Edited by: M. C. Facchini

References

Amato, F., Alastuey, A., Karanasiou, A., Lucarelli, F., Nava, S., Calzolai, G., Severi, M., Becagli, S., Gianelle, V. L., Colombi, C., Alves, C., Custódio, D., Nunes, T., Cerqueira, M., Pio, C., Eleftheriadis, K., Diapouli, E., Reche, C., Minguillón, M. C., Manousakas, M.-I., Maggos, T., Vratolis, S., Harrison, R. M., and Querol, X.: AIRUSE-LIFE+: a harmonized PM speciation and source apportionment in five southern European cities, Atmos. Chem. Phys., 16, 3289–3309, doi:10.5194/acp-16-3289-2016, 2016.

Atkinson, R., Baulch, D. L., Cox, R. A., Crowley, J. N., Hampson, R. F., Hynes, R. G., Jenkin, M. E., Rossi, M. J., and Troe, J.: Evaluated kinetic and photochemical data for atmospheric chemistry: Volume I – gas phase reactions of O_x, HO_x, NO_x and SO_x species, Atmos. Chem. Phys., 4, 1461–1738, doi:10.5194/acp-4-1461-2004, 2004.

Atkinson, R., Baulch, D. L., Cox, R. A., Crowley, J. N., Hampson, R. F., Hynes, R. G., Jenkin, M. E., Rossi, M. J., Troe, J., and IUPAC Subcommittee: Evaluated kinetic and photochemical data for atmospheric chemistry: Volume II – gas phase reactions of organic species, Atmos. Chem. Phys., 6, 3625–4055, doi:10.5194/acp-6-3625-2006, 2006.

Barker, M., Hengst, M., Schmid, J., Buers, H-J., Mittermaier, B., Klemp, D., and Koppmann, R.: Volatile organic compounds in the exhaled breath of young patients with cystic fibrosis, Eur. Respir. J., 275, 929–936, 2006.

Becker, K. H., Donner, B., and Gäb, S.: BERLIOZ: A field experiment within the German Tropospheric Research Programme, in: Proc. of EUROTRAC Symposium, edited by: P. M. Borrell and P. Borrell, 98, WIT-Press, Southhampton, 669–672, 1999.

Beekmann, M., Kerschbaumer, A., Reimer, E., Stern, R., and Möller, D.: PM measurement campaign HOVERT in the Greater Berlin area: model evaluation with chemically specified particulate matter observations for a one year period, Atmos. Chem. Phys., 7, 55–68, doi:10.5194/acp-7-55-2007, 2007.

Berlin Senate: Flächennutzung und Stadtstruktur, Senatsverwaltung für Stadtentwicklung, Berlin, 2010.

Berlin Senate: Ein Jahr Umweltzone Stufe 2 in Berlin, Senatsverwaltung für Stadtentwicklung, 38 pp., Berlin, 2011a.

Berlin Senate: 07.01 Verkehrsmengen (edition 2011), available at: http://www.stadtentwicklung.berlin.de/umwelt/umweltatlas/ic701.htm (last access: 23 September 2015), Berlin, Germany, 2011b.

Berlin Senate: Report 5, Green area information system (GrIS), Berlin, 2013a.

Berlin Senate: Luftreinhalteplan 2011–2017, Berlin, Germany, 2013b.

Berlin Senate: Senatsverwaltung für Gesundheit, Umwelt und Verbraucherschutz (Hrsg.): BLUME-Messnetz, available at: http://www.stadtentwicklung.berlin.de/umwelt/luftqualitaet/de/messnetz/, last access: 21 December 2015.

Birmili, W., Rehn, J., Vogel, A., Boehlke, C., Weber, K., and Rasch, F.: Micro-scale variability of urban particle number and mass concentrations in Leipzig, Germany, Meteorol. Z., 22, 155–165, 2013.

Blanchard, C. L., Hidy, G. M., Tanenbaum, S., Edgerton, E. S., and Hartsell, B. E.: The Southeastern Aerosol Research and Characterization (SEARCH) study: Spatial variations and chemical climatology, 1999–2010, J. Air Waste Manage., 63, 260–275, doi:10.1080/10962247.2012.749816, 2013.

Bonn, B.: Stress induced terpene emissions and new aerosol particle formation: A way of coniferous forests to mitigate climate feedback processes, Habilitation thesis, J.W. Goethe University, Frankfurt/Main, 2014.

Bonn, B. and Moortgat, G. K.: Sesquiterpene ozonolysis: Origin of atmospheric new particle formation from biogenic hydrocarbons, Geophys. Res. Lett., 30, 1585, doi:10.1029/2003GL017000, 2003.

Bonn, B., Butler, T., Churkina, G., Grote, R., Schäfer, K., Kerschbaumer, A., Nothard, R., von Stülpnagel, A., Hellen, H., and Hakola, H.: The influence of urban vegetation on urban air quality and particle mass: The BAERLIN2014 box model studies for Berlin, in preparation, 2016.

Bossard, M., Feranec, J., and Otahel, J.: CORINE Land Cover Technical Guide – Addendum, Tech. report 40, EEA, Copenhagen, Denmark, 2000.

Bourtsoukidis, E., Bonn, B., Dittmann, A., Hakola, H., Hellén, H., and Jacobi, S.: Ozone stress as a driving force of sesquiterpene emissions: a suggested parameterisation, Biogeosciences, 9, 4337–4352, doi:10.5194/bg-9-4337-2012, 2012.

Calfapietra, C., Fares, S., Manes, F., Morani, A., Sgrigna, G., and Loreto, F.: Role of Biogenic Volatile Organic Compounds (BVOC) emitted by urban trees on ozone concentration in cities: A review, Environ. Pollut., 183, 71–80, 2013.

Caplain, I., Cazier, F., Nouali, H., Mercier, A., Déchaux, J.-C., Nollet, V., Joumard, R., Andre, J.-M., and Vidon, R.: Emissions of unregulated pollutants from European gasoline and diesel passenger cars, Atmos. Environ., 40, 5954–5966, 2006.

Chambers, J. M., Cleveland, W. S., Kleiner, B., and Tukey, P. A.: Graphical Methods for Data Analysis, Wadsworth International Group, Belmont, USA, 1983.

Chen, B. and Kann, H.: Air pollution and population health: a global challenge, Environ. Health Prev. Med., 13, 94–101, doi:10.1007/s12199-007-0018-5, 2008.

Chen, D., Lia, Q., Stutz, J., Mao, Y., Zhang, L., Pikelnaya, O., Tsai, J. Y., Haman, C., Lefer, B., Rappenglück, B., Alvarez, S. L., Neuman, J. A., Flynn, J., Roberts, J. M., Nowake, J. B., de Gouw, J., Holloway, J., Wagner, N. L., Veres, P., Brown, S. S., Ryerson, T. B., Warneke, C., and Pollack, I. B.: WRF-Chem simulation of NO_x and O_3 in the L.A. basin during CalNex-2010, Atmos. Environ., 81, 421–432, doi:10.1016/j.atmosenv.2013.08.064, 2013.

Churkina, G., Grote, R., Butler, T. M., and Lawrence, M.: Natural selection? Picking the right trees for urban greening, Environ. Sci. Pol., 47, 12–17, 2015.

Collier, C. G.: The impact of urban areas on weather, Q. J. Roy. Meteor. Soc., 132, 1–25, 2006.

Cowling, E. B. and Furiness, C. (Eds.): The State of the Southern Oxidants Study (SOS) policy relevant findings in ozone and $PM_{2.5}$ pollution research 1995–2003, available at: https://www.ncsu.edu/sos/pubs/sos3/SOS-3TitleSec1.pdf (last access: 19 January 2016), 2004

Draxler, R. R. and Rolph, G. D.: HYSPLIT (Hybrid Single-Particle Lagrangian Integrated Trajectory), Model access via NOAA ARL READY, NOAA Air Resources Laboratory, Silver Spring, MD, 2013.

Dockery, D. W, Pope III, C. A., Xu, X., Spengler, J. D., Ware, J. H., Fay, F. E., Ferris Jr., B. G., and Speizer, F. E.: An association between air pollution and mortality in six U.S. cities, New Engl. J. Med., 329, 1753–1759, 1993.

Downey, N., Emery, C., Jung, J., Sakulyanontvittaya, T., Hebert, L., Blewitt, D., and Yarwood, G.: Emission reductions and urban ozone responses under more stringent US standards, Atmos. Environ., 101, 209–216, doi:10.1016/j.atmosenv.2014.11.018, 2015.

Dousset, B., Gourmelon, F., Laaidi, K., Zeghnoun, A., Giraudet, E., Bretin, P., Mauri, E., and Vandentorren, S.: Satellite monitoring of summer heat waves in the Paris metropolitan area, Int. J. Climatol., 31, 313–323, 2011.

ECJ (European Court of Justice): Case C237/07 Janecek v. Bayern, European Court of Justice, Judgement of 25 July 2008, available at: http://curia.europa.eu/juris/document/document.jsf;jsessionid=9ea7d0f130d51c7e0cbb16db4d2ab192e142ead63a73.e34KaxiLc3eQc40LaxqMbN4ObNeLe0?text=&docid=8148&pageIndex=0&doclang=EN&mode=lst&dir=&occ=first&part=1&cid=691454 (last access: 22 June 2016), 2008.

Ehlers, C.: Mobile Messungen – Messung und Bewertung von Verkehrsemissionen, PhD thesis, Cologne University, Cologne, Germany, 2013

Ehlers, C., Elbern, H., Klemp, D., Rohrer, F., and Wahner, A.: Comparison of measured data and model-results during PEGASOS-campaign 2012, Geophys. Res. Abstr., EGU2014-11591, EGU General Assembly 2014, Vienna, Austria, 2014.

Ehlers, C., Klemp, D., Rohrer, F., Mihelcic, D., Wegener, R., Kiendler-Scharr, A., and Wahner, A.: Twenty years of ambient observations of nitrogen oxides and specified hydrocarbons in air masses dominated by traffic emissions in Germany, Faraday Discuss., doi:10.1039/C5FD00180C, online first, 2015.

Ensberg, J. J., Hayes, P. L., Jimenez, J. L., Gilman, J. B., Kuster, W. C., de Gouw, J. A., Holloway, J. S., Gordon, T. D., Jathar, S., Robinson, A. L., and Seinfeld, J. H.: Emission factor ratios, SOA mass yields, and the impact of vehicular emissions on SOA formation, Atmos. Chem. Phys., 14, 2383–2397, doi:10.5194/acp-14-2383-2014, 2014.

European Committee for Standardisation (CEN): Workplace atmospheres – Size fraction definitions for measurement of airborne particles, CEN Standard EN 481, Brussels, 1993.

European Environmental Agency: Corine Land Cover 2006 raster data, Copenhagen, Denmark, available at: http://www.eea.europa.eu/data-and-maps/data/corine-land-cover-2006-raster-2 (last access: June 2015), 2012.

European Union: Directive no. 2008/50/EC of the European parliament and of the council on ambient air quality and cleaner air for Europe, Bruxelles, Belgium, 2008.

Fallmann, J., Emeis, S., and Suppan, P.: Mitigation of urban heat stress – a modelling case study for the area of Stuttgart, Die Erde, 144, 202–216, 2014.

Federal Administrative Court: Judgement of 16 August 2012, Doc. 7 C 21.12, available at: http://www.bverwg.de/entscheidungen/entscheidung.php?ent=050913U7C21.12.0 (last access: 22 June 2016), para. 41, 2012.

Fenner, D., Meier, F., Scherer, D., and Polze, A.: Spatial and temporal air temperature variability in Berlin, Germany, during the years 2001–2010, Urban Clim., 104, 308–331, 2014.

Finlayson, B. J. and Pitts Jr., J. N.: Chemistry of the upper and lower atmosphere, Academic Press, London, 2000.

Fischer, P. H., Marra, M., Ameling, C. B., Hoek, G., Beelen, R., de Hoogh, K., Breugelmans, O., Kruize, H., Janssen, N. A. H., and Houthuijs, D.: Air Pollution and Mortality in Seven Million Adults: The Dutch Environmental Longitudinal Study (DUELS), Environ. Health Persp., 123, 697–704, 2015

Folkers, A., Hüve, K., Ammann, C., Dindorf, T., Kesselmeier, J., Kleist, E., Kuhn, U., Uerlings, R., and Wildt, J.: Methanol emissions from deciduous tree species: dependence on temperature and light intensity, Plant Biol., 10, 65–75, 2008.

Ghirardo, A., Xie, J., Zheng, X., Wang, Y., Grote, R., Block, K., Wildt, J., Mentel, T., Kiendler-Scharr, A., Hallquist, M., Butterbach-Bahl, K., and Schnitzler, J.-P.: Urban stress-induced biogenic VOC emissions and SOA-forming potentials in Beijing, Atmos. Chem. Phys., 16, 2901–2920, doi:10.5194/acp-16-2901-2016, 2016.

Grewe, D., Thompson, H. L., Salmond, J. A., Cai, X. M., and Schlünzen, K. H.: Modelling the impact of urbanisation on regional climate in the Greater London Area, Int. J. Climatol., 33, 2388–2401, 2013.

Griffin, R. J., Cocker III, D. R., Seinfeld, J. H., and Dabdub, D.: Estimate of global atmospheric organic aerosol from oxidation of biogenic hydrocarbons, Geophys. Res. Lett., 26, 2721–2724, doi:10.1029/1999GL900476, 1999.

Guenther, A., Hewitt, C. N., Erickson, D., Fall, R., Geron, C., Graedel, T., Harley, P., Klinger, L., Lerdau, M., McKay, W. A., Pierces, T., Scholes, B., Steinbrecher, R., Tallamraju, R., Taylor, J., and Zimmerman, P.: A global model of natural volatile organic compound emissions, J. Geophys. Res., 100, 8873–8892, 1995.

Guenther, A., Karl, T., Harley, P., Wiedinmyer, C., Palmer, P. I., and Geron, C.: Estimates of global terrestrial isoprene emissions using MEGAN (Model of Emissions of Gases and Aerosols from Nature), Atmos. Chem. Phys., 6, 3181–3210, doi:10.5194/acp-6-3181-2006, 2006.

Hallquist, M., Wenger, J. C., Baltensperger, U., Rudich, Y., Simpson, D., Claeys, M., Dommen, J., Donahue, N. M., George, C., Goldstein, A. H., Hamilton, J. F., Herrmann, H., Hoffmann, T., Iinuma, Y., Jang, M., Jenkin, M. E., Jimenez, J. L., Kiendler-Scharr, A., Maenhaut, W., McFiggans, G., Mentel, Th. F., Monod, A., Prévôt, A. S. H., Seinfeld, J. H., Surratt, J. D., Szmigielski, R., and Wildt, J.: The formation, properties and impact of secondary organic aerosol: current and emerging issues, Atmos. Chem. Phys., 9, 5155–5236, doi:10.5194/acp-9-5155-2009, 2009.

Heinrich, J., Thiering, E., Rzehak, P., Krämer, U., Hochadel, M., Rauchfuss, K. M., Gehring, U., Wichmann, H. E.: Long-term exposure to NO_2 and PM_{10} and all-cause and cause-specific mortality in a prospective cohort of women, Occup. Environ. Med., 70, 179–186, 2013.

Henschel, S., Le Tertre, A., Atkinson, R. W., Querol, X., Pandolfi, M., Zeka, A., Haluza, D., Analitis, A., Katsouyanni, K., Bouland, C., Pascal, M., Medina, S., and Goodman, P. G.: Trends of nitrogen oxides in ambient air in nine European cities between 1999 and 2010, Atmos. Environ., 117, 234–241, 2015.

Holst, T., Ameth, A., Hayward, S., Ekberg, A., Mastepanov, M., Jackowicz-Korczyñski, M., Friborg, T., Crill, P. M., and Bïckstrand, K.: BVOC ecosystem flux measurements at a high latitude wetland site, Medd. Lunds Universitets Geografiska Institutioner, 184, 69–82, 2009.

Hong, A., Schweitzer, L., Yang, W., and Marr, L. C.: Impact of Temporary Freeway Closure on Regional Air Quality: A Lesson from Carmageddon in Los Angeles, United States, Environ. Sci. Technol., 49, 3211–3218, doi:10.1021/es505185c, 2015.

Huang, J., Liu, H., Crawford, J. H., Chan, C., Considine, D. B., Zhang, Y., Zheng, X., Zhao, C., Thouret, V., Oltmans, S. J., Liu, S. C., Jones, D. B. A., Steenrod, S. D., and Damon, M. R.: Origin of springtime ozone enhancements in the lower troposphere over Beijing: in situ measurements and model analysis, Atmos. Chem. Phys., 15, 5161–5179, doi:10.5194/acp-15-5161-2015, 2015.

Huo, H., Cai, H., Zhang, Q., Liu, F., and He, K.: Life-cycle assessment of greenhouse gas and air emissions of electric vehicles: A comparison between China and the U.S., Atmos. Environ., 108, 107–116, doi:10.1016/j.atmosenv.2015.02.073, 2015.

Hüve, K., Christ, M., Kleist, E., Uerlings, R., Niinemets, U., Walter, A., and Wildt, J.: Simultaneous growth and emission measurements demonstrate an interactive control of methanol release by leaf expansion and stomata, J. Exp. Bot., 58, 1783–1793, 2007.

Irga, P. J., Burchett, M. D., and Torpy, F. R.: Does urban forestry have a quantitative effect on ambient air quality in an urban environment?, Atmos. Environ., 120, 173–181, doi:10.1016/j.atmosenv.2015.08.050, 2015.

Janhäll, S.: Review on urban vegetation and particle air pollution – Deposition and dispersion, Atmos. Environ., 105, 130–137, 2015.

Jedynska, A., Tromp, P. C., Houtzager, M. M. G., and Kooter, I. M.: Chemical characterization of biofuel exhaust emissions, Atmos. Environ., 116, 172–182, 2015.

Jones, P. D. and Lister, D. H.: The urban heat island in Central London and urban-related warming trends in Central London since 1900, Weather, 64, 323–327, 2009.

Junkermann, W.: The actinic UV-radiation budget during the ESCOMPTE campaign 2001: Results of airborne measurements with the microlight research aircraft D-MIFU, Atmos. Res., 74, 461–475, doi:10.1016/j.atmosres.2004.06.009, 2005.

Junkermann, W., Hagemann, R., and Vogel, B.: Nucleation in the Karlsruhe plume during the COPS/TRACKS-Lagrange experiment, Q. J. Royal Meteor. Soc., 137, 267–274, 2011.

Junkermann, W., Vogel, B., and Bangert, M.: Ultrafine particles over Germany – an aerial survey, Tellus B, 68, 29250, doi:10.3402/tellusb.v68.29250, 2016.

Kaminski, H., Kuhlbusch, T. A. J., Rath, S., Götz, U., Sprenger, M., Wels, D., Polloczek, J., Bachmann, V., Dziurowitz, N., Kiesling, H.-J., Schwiegelshohn, A., Monz, C., Dahmann, D., and Asbach, C.: Comparability of mobility particle sizers and diffusion chargers, J. Aerosol Sci., 57, 156–178, 2013.

Kerschbaumer, A.: On the aerosol budget over Berlin, PhD thesis, Free University, Berlin, 2007.

Keskinen, J., Pietarinen, K., and Lehtimäki, M.: Electrical Low Pressure Impactor, J. Aerosol Sci., 23, 353–360, 1992.

Kiesewetter, G., Borken-Kleefeld, J., Schöpp, W., Heyes, C., Thunis, P., Bessagnet, B., Terrenoire, E., Fagerli, H., Nyiri, A., and Amann, M.: Modelling street level PM_{10} concentrations across Europe: source apportionment and possible futures, Atmos. Chem. Phys., 15, 1539–1553, doi:10.5194/acp-15-1539-2015, 2015.

Klemp, D., Mihelcic, D., and Mittermaier, B.: Messung und Bewertung von Verkehrsemissionen. Series for Energy & Environment, Schriften des Forschungszentrums Jülich, 21, Jülich, Germany, ISBN:978-3-89336-546-3, 2012.

Kofahl, C.: Hochempfindliche Bestimmung der organischen und anorganischen Kohlenstoff-Fraktion in Feinstaubproben mittels CRD-Spektroskopie, Bachelor thesis, University of Applied Sciences, Aachen, 2012.

Kreuzwieser, J., Kühnemann, F., Martis, A., Rennenberg, H., and Urbau, W.: Diurnal pattern of acetaldehyde emission by flooded poplar trees, Plant Physiol., 108, 79–86, 2000.

Kulmala, M., Dal Maso, M., Mäkelä, J. M., Pirjola, L., Väkevä, M., Aalto, P., Miikkulainen, P., Hämeri, K., and O'Dowd, C. D.: On the formation, growth and composition of nucleation mode particles, Tellus B, 53, 479–490, 2001.

Lamsal, L. N., Martin, R. V., Parrish, D. D., and Krotkov, N. A.: Scaling Relationship for NO_2 Pollution and Urban Population Size: A Satellite Perspective, Environ. Sci. Technol., 47, 7855–7861, doi:10.1021/es400744g, 2013.

Lehtinen, K. E. J. and Kulmala, M.: A model for particle formation and growth in the atmosphere with molecular resolution in size, Atmos. Chem. Phys., 3, 251–257, doi:10.5194/acp-3-251-2003, 2003.

Lelieveld, J., Evans, J. S., Fnais, M., Giannadaki, D., and Pozzer, A.: The contribution of outdoor air pollution sources to premature mortality on a global scale, Nature, 525, 367–371, doi:10.1038/nature15371, 2015.

Li, T., Izumi, H., Shudo, T., and Ogawa, H.: Characteristics of unregulated toxic emissions from ultra-high EGR low temperature diesel combustion and effects of exhaust catalysts, T. Jpn. Soc. Mechan. Eng., Part B, 73, 1129–1134, 2007.

Liu, W.-T., Lee, K.-Y., Lee, H.-C., Chuang, H.-C., Wug, D., Juang, J.-N., and Chuang, K.-J.: The association of annual air pollution exposure with blood pressure among patients with sleep-disordered breathing, Sci. Total Environ., 543, 61–66, 2016.

MacDonald, R. and Fall, R.: Detection of substantial emissions of methanol from plants to the atmosphere, Atmos. Environ. A-Gen., 27, 1709–1713, 1993.

Mancilla, Y., Mendoza, A., Fraser, M. P., and Herckes, P.: Organic composition and source apportionment of fine aerosol at Monterrey, Mexico, based on organic markers, Atmos. Chem. Phys., 16, 953–970, doi:10.5194/acp-16-953-2016, 2016.

McDonald, B. C., Goldstein, A. H., and Harley, R. A.: Long-term trends in California mobile source emissions and ambient concentrations of black carbon and organic aerosol, Environ. Sci. Technol., 49, 5178–5188, doi:10.1021/es505912b, 2015.

Padilla, C. M., Kihal-Talantikite, W., Vieira, V. M., Rossello, P., Nir, G. L., Zmirou-Navier, D., and Deguen, S.: Air quality and social deprivation in four French metropolitan areas-A localized spatio-temporal environmental inequality analysis, Environ. Res., 134, 315–324, doi:10.1016/j.envres.2014.07.017, 2014.

Papiez, M. R., Potosnak, M. J., Goliff, W. S., Guenther, A. B., Matsunaga, S. N., and Stockwell, W. R.: The impacts of reactive terpene emissions from plants on air quality in Las Vegas, Nevada, Atmos. Environ., 43, 4109–4123, 2009.

Peng, R. D., Dominici, F., Pastor-Barriuso, R., Zeger, S. L., and Samet, J. M.: Seasonal analyses of air pollution and mortality in 100 US cities, Am. J. Epidemiol., 161, 585–594, 2005.

Petit, J.-E., Favez, O., Sciare, J., Canonaco, F., Croteau, P., Mocnik, G., Jayne, J., Worsnop, D., and Leoz-Garziandia, E.: Submicron aerosol source apportionment of wintertime pollution in Paris, France by double positive matrix factorization (PMF^2) using an aerosol chemical speciation monitor (ACSM) and a multi-wavelength Aethalometer, Atmos. Chem. Phys., 14, 13773–13787, doi:10.5194/acp-14-13773-2014, 2014.

Pope III, C. A., Ezzati, M., and Dockery, D. W.: Fine-particulate air pollution and life expectancy in the United States, New Engl. J. Med., 360, 376–386, 2009.

Sakulyanontvittaya, T., Guenther, A., Helmig, D., Milford, J., and Wiedinmyer, C.: Secondary organic aerosol from sesquiterpene and monoterpene emissions in the United States. Environ. Sci. Technol., 42, 8784–8790, doi:10.1021/es800817r, 2008.

Schmitz, Th., Hassel, D., and Weber, F. J.: Determination of VOC-components in the exhaust of gasoline and diesel passenger cars, Atmos. Environ., 34, 4639–4647, 2000.

Schubert, S. and Grossman-Clarke, S.: The Influence of green areas and roof albedos on air temperatures during Extreme Heat Events in Berlin, Germany, Meteorol. Z., 22, 131–143, 2013.

Seinfeld, J. H. and Pandis, S. N.: Atmospheric chemistry and physics, From air pollution to climate change, 2nd Edn., Wiley Interscience, Oxford, 2006.

Shahraiyni, H. T., Sodoudi, S., Kerschbaumer, A., and Cubasch, U.: A new structure identification scheme for ANFIS and its application for the simulation of virtual air pollution monitoring stations in urban areas, Eng. Appl. Artif. Intel., 41, 175–182, doi:10.1016/j.engappai.2015.02.010, 2015a.

Shahraiyni, H. T., Sodoudi, S., Kerschbaumer, A., and Cubasch, U.: New Technique for Ranking of Air Pollution Monitoring Stations in the Urban Areas Based upon Spatial Representativity (Case Study: PM Monitoring Stations in Berlin), Aerosol Air Qual. Res., 15, 743–748, doi:10.4209/aaqr.2014.12.0317, 2015b.

Situ, S., Guenther, A., Wang, X., Jiang, X., Turnipseed, A., Wu, Z., Bai, J., and Wang, X.: Impacts of seasonal and regional variability in biogenic VOC emissions on surface ozone in the Pearl River delta region, China, Atmos. Chem. Phys., 13, 11803–11817, doi:10.5194/acp-13-11803-2013, 2013.

Sua, C., Hampel, R., Franck, U., Wiedensohler, A., Cyrysa, J., Pane, X., Wichmann, H.-E., Peters, A., Schneider, A., and Breitner, S.: Assessing responses of cardiovascular mortality to particulate matter air pollution for pre-, during- and post-2008 Olympics periods, Environ. Res., 142, 112–122, doi:10.1016/j.envres.2015.06.025, 2015.

Setälä, H., Viippola, V., Rantalainen, A.-L., Pennanen, A., and Yli-Pelkonen, V.: Does urban vegetation mitigate air pollution in northern conditions?, Environ. Pollut., 183, 104–112, 2013.

Stojić, A., Stojić, S. S., Šoštarić, A., Ilić, L., Mijić, Z., and Rajšić, S.: Characterization of VOC sources in an urban area based on PTR-MS measurements and receptor modelling, Environ. Sci. Pollut. R., 22, 13137–13152, 2015.

Tullius, K. and Lutz, M. (Eds.): Healthier Environment through the Abatement of Vehicle Emissions and Noise (HEAVEN) final report, EU project-no. IST-1999-11244, Bruxelles, Belgium, 2003.

UFIREG UltraFIne Particles – an evidence based contribution to the development of REGional and European environmental and health policy: Data collection and methods, Report, project no. 3CE288P3, European Union, Bruxelles, available at: http://www.ufireg-central.eu/index.php/downloads (last access: 24 September 2015), 2014.

United Nations: Department of Economics and Social Affairs, available at: http://www.geohive.com/earth/population_now.aspx, last access: 16 July 2015.

Valach, A. C., Langford, B., Nemitz, E., MacKenzie, A. R., and Hewitt, C. N.: Seasonal and diurnal trends in concentrations and fluxes of volatile organic compounds in central London, Atmos. Chem. Phys., 15, 7777–7796, doi:10.5194/acp-15-7777-2015, 2015.

Van den Bossche, J., Peters, J., Verwaeren, J., Botteldooren, D., Theunis, J., and De Baets, B.: Mobile monitoring for mapping spatial variation in urban air quality: Development and validation of a methodology based on an extensive dataset, Atmos. Environ., 105, 148–161, 2015.

Van Poppel, M., Peters, J., and Bleux, N.: Methodology for setup and data processing of mobile air quality measurements to assess the spatial variability of concentrations in urban environments, Environ. Pollut., 183, 224–233, 2013.

Velikova, V., Pinelli, P., Pasqualini, S., Reale, L., Ferranti, F., Loreto, F.: Isoprene decreases the concentration of nitric oxide in leaves exposed to elevated ozone, New Phytol., 166, 419–426, 2005.

von der Weiden-Reinmüller, S.-L., Drewnick, F., Zhang, Q. J., Freutel, F., Beekmann, M., and Borrmann, S.: Megacity emission plume characteristics in summer and winter investigated by mobile aerosol and trace gas measurements: the Paris metropolitan area, Atmos. Chem. Phys., 14, 12931–12950, doi:10.5194/acp-14-12931-2014, 2014.

von Schneidemesser, E., Monks, P. S., Gros, V., Gauduin, J., and Sanchez, O.: How important is biogenic isoprene in an urban environment? A study in London and Paris, Geophys. Res. Lett., 38, L19804, doi:10.1029/2011GL048647, 2011.

von Schneidemesser, E., Bonn, B., Schmale, J., Gerwig, H., Lüdecke, A., Kura, J., Pietsch, A., Schäfer, K., Ehlers, C., Kofahl, C., Klemp, D., Nothard, R., von Stülpnagel, A., Kerschbaumer, A., Churkina, G., Grote, R., Otero Felipe, N., Quedenau, J., But-

ler, T., and Lawrence, M. G.: BAERLIN2014 – gas-phase and particle measurements and source apportionment at an urban background site in Berlin, in preparation, 2016.

von Stülpnagel, A., Kaupp, H., and Nothard, R.: Luftgütemessdaten 2014, Department for urban development and environment, Berlin, Germany, 2015.

Warneke, C., Karl, T., Judmaier, H., Hansel, A., Jordan, A., Lindinger, W., and Crutzen, P. J.: Acetone, methanol, and other partially oxidized volatile organic emissions from dead plant matter by abiological processes: Significance for atmospheric HO_x chemistry, Global Biogeochem. Cy., 13, 9–17, 1999.

Waser, L. T. and Schwarz, M.: Comparison of large-area land cover products with national forest inventories and CORINE land cover in the European Alps, Int. J. Appl. Earth Obs., 8, 196–207, 2006.

Weber, K., Eliasson, J., Vogel, A., Fischer, C., Pohl, T., van Haren, G., Meier, M., Grobéty, B., and Dahmann, D.: Airborne in-situ investigations of the Eyjafjallajökull volcanic ash plume on iceland and over north-western Germany with light aircrafts and optical particle counters, Atmos. Environ., 48, 9–21, 2012.

World Health Organisation: Air quality guidelines for particulate matter, ozone, nitrogen dioxide and sulfur dioxide – Global update 2005 – Summary of risk assessment, Geneva, Switzerland, 2006.

World Health Organisation: Review of Evidence on Health Aspects on Air Pollution e REVIHAAP Project, Technical Report, WHO Regional Office for Europe, Copenhagen, Denmark, available at: http://www.euro.who.int/__data/assets/pdf_file/0004/193108/REVIHAAP-Final-technical-report.pdf (last access: 22 June 2016), 2013.

Zaveri, R. A., Shaw, W. J., Cziczo, D. J., Schmid, B., Ferrare, R. A., Alexander, M. L., Alexandrov, M., Alvarez, R. J., Arnott, W. P., Atkinson, D. B., Baidar, S., Banta, R. M., Barnard, J. C., Beranek, J., Berg, L. K., Brechtel, F., Brewer, W. A., Cahill, J. F., Cairns, B., Cappa, C. D., Chand, D., China, S., Comstock, J. M., Dubey, M. K., Easter, R. C., Erickson, M. H., Fast, J. D., Floerchinger, C., Flowers, B. A., Fortner, E., Gaffney, J. S., Gilles, M. K., Gorkowski, K., Gustafson, W. I., Gyawali, M., Hair, J., Hardesty, R. M., Harworth, J. W., Herndon, S., Hiranuma, N., Hostetler, C., Hubbe, J. M., Jayne, J. T., Jeong, H., Jobson, B. T., Kassianov, E. I., Kleinman, L. I., Kluzek, C., Knighton, B., Kolesar, K. R., Kuang, C., Kubátová, A., Langford, A. O., Laskin, A., Laulainen, N., Marchbanks, R. D., Mazzoleni, C., Mei, F., Moffet, R. C., Nelson, D., Obland, M. D., Oetjen, H., Onasch, T. B., Ortega, I., Ottaviani, M., Pekour, M., Prather, K. A., Radney, J. G., Rogers, R. R., Sandberg, S. P., Sedlacek, A., Senff, C. J., Senum, G., Setyan, A., Shilling, J. E., Shrivastava, M., Song, C., Springston, S. R., Subramanian, R., Suski, K., Tomlinson, J., Volkamer, R., Wallace, H. W., Wang, J., Weickmann, A. M., Worsnop, D. R., Yu, X.-Y., Zelenyuk, A., and Zhang, Q.: Overview of the 2010 Carbonaceous Aerosols and Radiative Effects Study (CARES), Atmos. Chem. Phys., 12, 7647–7687, doi:10.5194/acp-12-7647-2012, 2012.

Zhang, Z., Zhang, X., Gong, D., Quan, W., Zhao, X., Ma, Z., and Kim, S.-J.: Evolution of surface O_3 and $PM_{2.5}$ concentrations and their relationships with meteorological conditions over the last decade in Beijing, Atmos. Environ., 108, 67–75, 2015.